UNIVERSITY OF CAPE TOWN

Consistency and convergence of SPH approximations

by

Karl Penzhorn

A thesis submitted in partial fulfillment for the
degree of Master of Science in Engineering

in the
Faculty of Engineering and the Built Environment
Centre for Research in Computational and Applied Mechanics

October 2009

Declaration of Authorship

I, KARL PENZHORN, declare that this thesis titled, 'CONSISTENCY AND CONVERGENCE OF SPH APPROXIMATIONS' and the work presented in it are my own. I confirm that:

- This work was done wholly or mainly while in candidature for a research degree at this University.
- Where any part of this thesis has previously been submitted for a degree or any other qualification at this University or any other institution, this has been clearly stated.
- Where I have consulted the published work of others, this is always clearly attributed.
- Where I have quoted from the work of others, the source is always given. With the exception of such quotations, this thesis is entirely my own work.
- I have acknowledged all main sources of help.
- Where the thesis is based on work done by myself jointly with others, I have made clear exactly what was done by others and what I have contributed myself.

Signed: _____

Date: _____

"When the facts change, I change my mind. What do you do, sir?"

John Maynard Keynes

UNIVERSITY OF CAPE TOWN

Abstract

Faculty of Engineering and the Built Environment
Centre for Research in Computational and Applied Mechanics

Master of Science in Engineering

by Karl Penzhorn

Smoothed particle hydrodynamics, or SPH, is a technique for solving differential equations numerically. This thesis is about a new approach to SPH. Instead of using a single kernel or shape function for approximation of a function and its derivatives, individual shape functions are used for each derivative. The investigation is carried out in one space dimension. After producing the conditions for consistency and convergence for the zeroth, first and second derivatives, a new set of linear or piecewise-linear shape functions which meet the minimum of these requirements are presented for each. The properties of the subsequent approximations are then examined in the context of (a) approximation of functions and (b) SPH approximations to the advection-diffusion equation. These are compared with results obtained using the standard SPH method with conventional shape functions. Standard SPH shape functions which with their derivatives meet the conditions developed are also presented. Particular attention is paid to the conditions under which solutions will converge with respect to both particle density and shape function support. This leads to some revelations on problems with SPH implementations in the literature, including the methods used to extend the problem domain in order to mitigate truncation near the boundary, and the sensitivity of results with regard to the number of particles used in integrating shape functions.

Chapter 1

Introduction

1.1 What is SPH?

Smoothed particle hydrodynamics, or SPH, is a technique for solving differential equations numerically. The method is based on the replacement of the unknown function and its derivatives by smoothed approximations, and the discretisation of the smoothing approximations by an appropriate quadrature scheme.

In one space dimension, given a function f and an auxiliary function W (called the *shape function*, the *weighting function* or the *kernel*), the smoothed approximation $< f >$ of f can be written as

$$< f > (x) = \int_a^b f(\xi)\, W(\xi - x, r)\; d\xi \quad , \tag{1.1}$$

where r is the support of W and W is chosen such that $< f > (x) \to f(x)$ as $r \to 0$ (more on how this is done in Chapter 2). The approximation of the derivative of f then follows in the same way from

$$< f' > (x) = \int_a^b f'(\xi)\, W(\xi - x, r)\; d\xi\,. \tag{1.2}$$

Using integration by parts this becomes

$$< f' > (x) = \Big[\; f(\xi) W(\xi - x, r) \;\Big]_{\xi=a}^{b} - \int_a^b f(\xi)\, W'(\xi - x, r)\; d\xi\,. \tag{1.3}$$

If we now ensure that

$$W(a - x, r) = W(b - x, r) = 0 \tag{1.4}$$

then (1.3) becomes

$$< f' > (x) = - \int_a^b f(\xi)\, W'(\xi - x, r)\ d\xi \quad . \tag{1.5}$$

This process can be repeated to get

$$< f'' > (x) = \int_a^b f(\xi)\, W''(\xi - x, r)\ d\xi \tag{1.6}$$

so long as $W'(a-x,r) = W'(b-x,r) = 0$. Thus, so long as we ensure that $< f > \rightarrow f$ in some way, the derivatives of f can be formulated in terms of its values and the derivatives of W, using this approach. Indeed, the weighting functions are chosen in such a way as to ensure that this condition is satisfied.

In the same way smoothed approximations of f and its derivatives may be constructed in higher space dimensions. These approximations may be used to construct approximate solutions to differential equations, in which the derivatives are replaced by discrete approximations to give a system of discrete simultaneous equations, which is easily solved.

Thus SPH is similar in form to interpolation methods which also replace f with an approximate function for which derivatives are readily available. The difference is that SPH does not enforce collocation or even error minimisation but instead uses direct integrals for its evaluations. This makes the method very simple to implement, which is one of its most salient features.

1.2 Origins of SPH

SPH was proposed independently in 1977 by astrophysicists Lucy [1], Gingold and Monaghan [2] and also by Liszka [3] as a way to solve the equations for fluid flow numerically. Originally used as a straightforward way to model the rapid motion of certain astrophysical phenomena such as star formation, it has undergone many improvements and adaptations and has been applied to problems in both fluid and solid mechanics. Starting in the 1990s it started to raise the interest of researchers in areas of mechanics involving high deformation rates such as shock loading (see, for example, [21] and [17]), material fracture and separation (see [25] and [26]), and mixing (see [27] and [28]). The lack of prescribed connectivity between information points and the lack of a fixed background spatial grid meant that issues arising from mesh distortion were moot.

1.3 Fundamental understanding of SPH

SPH has not seen widespread attention outside of certain select fields of inquiry (i.e. astrophysics and solid mechanics), possibly because it does not have the same rigorous foundation as do methods such as the Galerkin finite element method, or indeed a host of Galerkin meshless methods such as the Element Free Galerkin method [29]. Babuška [22], in an overview of meshless methods, identified over 200 engineering papers and four books in the field, and presents the view that the literature consists mostly of heuristic experience with little fundamental, mathematical understanding of applicability and performance. Examples of this absence of a rigorous foundation are the absence of verification of the assumptions used to select shape functions, and in the case of SPH, the absence of a complete convergence theory. This would be in contrast to approaches such as the Generalised Finite Element Method [30], which does rest on a solid theoretical foundation.

One aim of this thesis is to address some of these issues, and to gain a better understanding of how SPH works. Specifically we are interested in whether our approximations converge, that is, that the approximations tend to a limit as the relevant parameters become smaller, and whether our approximations are consistent, that is, that the limit to which they converge is the solution to the original problem.

There have been recent works which address this set of issues in the context of SPH. Two key contributions are those of Laguna [24] and Quinlan et al. [20].

In 1995 Laguna set out to use SPH to solve non-hydrodynamical problems. Up until this point assumptions had been made about the meaning of the discretisation of the SPH integrals, an interpretation being that each information point represented a portion of the mass of the substance being modelled. That is, in order to evaluate the integral

$$<f>(x) = \int f(\xi)\, W(\xi - x, r)\; dV \tag{1.7}$$

one would write

$$<f>(x) \;\approx\; \sum_j f(x_j)\, W(x_j - x, r)\, \frac{m_j}{\rho_j} \tag{1.8}$$

where m_j is the mass of particle j and ρ_j is the density, since in a system where each information point represents a fraction of the total mass one could write $\Delta V \equiv m_j/\rho_j$. Laguna, however, did not assume that the information points represented masses but rather that they were regions in which field variables are known or sought, and so developed a general technique for evaluating weighted integrals. With smoothing approximations of functions and their gradients in terms of only arbitrary field variables,

one could look at how SPH would operate as a scheme that solved general hyperbolic and parabolic equations.

Laguna started by testing the quality of SPH approximations (which he called SPI, Smoothed Particle Interpolation) applied to functions such as $\sin x$, and also approximations of their first and second derivatives, examining the error both with regard to sampling resolution, that is, the number of points used to discretise the problem domain, and size of the shape function cover, a fundamental consideration when performing smoothed approximations. In his analysis he finds that in order for the error to converge $h^{-n}(\Delta x/h)^2 \to 0$ as Δx and $h \to 0$, where n is the derivative being approximated. That is, convergence is only achieved when the sampling resolution under the cover, i.e. $(\Delta x/h)$, increases faster than the shape function cover decreases.

Details of implementation in the paper are sparse in certain respects. For example, we do not know how boundaries were treated, that is, whether the domain of the function being approximated was extended beyond the test domain in order not to have to deal with shape function truncation, and if so, how. This is an important consideration in this thesis and we look at various ways to extend the test domain.

In later chapters we will report on similar tests, using a modified SPH formulation. Also, we look at both the SPH approximation of derivatives and the use of those approximations to solve boundary value problems.

In 2005 Quinlan et al. [20] carried out a detailed study of the error arising from both the smoothing integral and its discretisation. The error at a point x arising from the integral, called the smoothing error, is defined by

$$e_s(x) = \left| f(x) - <f>(x) \right| \tag{1.9}$$

$$= \left| f(x) - \int f(\xi)\, W(\xi - x, r)\, d\xi \right| \tag{1.10}$$

and is shown to depend on r. For example, one can show that for a cubic spline shape function the smoothing error is $O(r^2)$, and for a super-gaussian the error is $O(r^4)$ (see [31] for more). Another error is introduced through the discretisation of the integral which is, as Quinlan et al. show, very often the dominant error in SPH approximations. These authors use the rectangular rule, also known as the midpoint rule, and find that with uniform spacing the discretisation error, defined by

$$e_d(x) = \left| <f>(x) \; - \; \widehat{<f>}(x) \right|$$

$$= \left| \int f(\xi)\, W(\xi - x, r)\; d\xi \; - \; \sum_j f(x_j)\, W(x_j - x, r)\, \Delta x \right| \quad , \tag{1.11}$$

where Δx is the particle spacing, is proportional to $(\Delta x/r)^{\beta+2}$ and another term involving r^2, where β is the highest integer such that the βth derivative and all lower derivatives of W are zero at the edges of the compact support. Thus as $\Delta x/r$ is reduced the error becomes limited by the smoothness of the shape function at the boundary. Similarly, it is not sufficient to reduce r without also reducing the particle spacing. Quinlan et al. perform tests on sinusoids of varying wavelengths and magnitudes and find good agreement with the theory developed in the paper.

In this thesis we will be testing not just function approximation but also the solution to boundary value problems. We restrict our work to uniform particle spacing in order to focus on the problems of convergence and the properties of shape functions that lead to convergent behaviour.

While the works by Laguna and by Quinlan et al. have been central to the investigations reported in this thesis, there are several others which have contributed to the fundamental understanding of SPH.

In 1982 Monaghan, one of the inventors of SPH, wrote a paper entitled "Why Particle Methods Work" [31]. In it he tries to account for the ability of SPH integrals to approximate functions and their gradients. To this end he uses Taylor expansion of the SPH function approximation $< f >$ to show that $O(r^n), n = 1, 2, ...$, accuracy can be achieved through correct shape function selection. In our work we use the same technique to establish conditions under which we can achieve consistency when approximating derivatives, i.e. $< f' >$ and $< f'' >$.

In 1996 Johnson and Beissel [16] proposed normalising the smoothing function which ensured first-order consistency near a boundary.

In 1996 Belytschko et al. [18] showed under which conditions the first derivative is consistent and in 1998 [19] reviewed various methods proposed to achieve it.

In 1999 Chen et al. [5] used Taylor expansion to provide a new way to derive the SPH integrals in order to resolve issues arising near the boundary. In this work they briefly suggest that separate shape functions could be used for each derivative but do not investigate the possibility further. In their tests they consider $< f >$, $< f' >$ and $< f'' >$ for basic polynomial functions.

Finally, in 2002 Bonet and Kulasegaram [35] looked at the accuracy and stability of function and gradient approximations, viewing SPH as a generic interpolation technique much as in [20] and [24]. They propose a kernel correction technique to ensure linear consistency and use their method to solve a Poisson-type differential equation. They find that the linear correction alone is not sufficient to achieve an accurate solution and

consequently investigate the role of quadrature in the consistency of SPH approximations. From this they develop an integration correction technique which improves their results. They then go on to discuss stabilisation issues arising from zero-energy modes and propose a technique to mitigate these issues, showing promising results.

Several papers have also taken an experimental approach to ascertaining the characteristics of SPH approximations. In 1996 Fulk and Quinn [4] performed a study on the effectiveness of various shape functions in function reproduction, focusing on the results of tests and various error measures on them. They find that bell-shaped shape functions performed best. In 2003 Hongbin and Xin [32] performed a similar study but also looked at the production of derivatives and conclude that Gaussian and Q-spline shape functions are to be preferred. In 2008 Cabezn et al. [33] went further by looking at a whole family of shape functions and their performance with regard to the second derivative, the case of disordered particles and approximations in two dimensions.

In contrast to these works, this thesis will focus on the conditions under which SPH approximations are consistent and converge, rather than which shape functions perform the best.

1.4 Aims of this thesis

There is still no general theory which explains and prescribes conditions for consistency and convergence in SPH. In this thesis we propose to provide such a framework for the simple case of one space dimension with evenly spaced nodes. We show which conditions are required for consistency and convergence of any derivative, propose a technique for achieving said conditions for the zeroth, first and second derivatives, and provide some test results which confirm our assertions.

The structure of the rest of this work is as follows.

In Chapter 2 we present the standard SPH method, giving details on the conditions prescribed on shape functions and giving examples of shape functions frequently used. We then use Taylor expansion to ascertain, for each derivative separately, the conditions under which consistency and convergence will be achieved. We then look at whether the conditions prescribed in the standard SPH method imply the consistency and convergence conditions developed. A new approach to SPH is then presented in which the shape functions are chosen for each derivative separately, satisfying the minimum of the developed conditions. We then look at the issue of shape function truncation near the boundary, looking at the conditions under which approximations will be consistent when extending the function at the boundaries in some way. Boundary conditions and

their relevance to the work in this thesis are discussed. Finally numerical integration is discussed, and the Euler-Maclaurin formula is used to estimate the discretisation error when using the rectangular rule to approximate smoothing integrals.

Chapter 3 is concerned with the advection-diffusion equation, the model differential equation used in this work. This equation has attracted much interest in the numerical analysis community because of the difficulties associated with obtaining stable approximations in advection-dominated situations. It is thus a good choice of model problem. Properties of the solution to this equation are presented, and various existing approaches to obtaining approximate solutions are summarised.

In Chapter 4 we present the results of numerical experiments carried out to test the theory in Chapter 2. We first explain the technique used to extend functions at the boundaries in a way which satisfies the consistency conditions developed. We then detail the various quadrature techniques used. The tests involving the approximation of functions and their derivatives follow, ending finally with tests which solve the advection-diffusion equation.

Finally in Chapter 5 we summarise the work of the entire thesis and present the conclusions that are found most pertinent to the goals of the work, whilst also presenting suggestions for further work.

Chapter 2

SPH

This chapter starts with an overview of the standard approach to SPH, in one space dimension. The overview includes a discussion of the choice of kernel or shape function. This is followed by an analysis of the conditions for consistency of smoothed approximations, using Taylor series expansions. We then address the question of whether the shape functions used in the SPH literature meet these conditions.

The next section is devoted to a presentation of new, simple shape functions which are constructed specifically to satisfy the consistency conditions developed previously. Different shape functions are designed for functions, their first and second derivatives, as opposed to traditional SPH which uses one shape function.

The issue of domain extension is discussed next, discussing the need for it and the conditions under which it does not break consistency. This is followed with a discussion on imposing boundary conditions and how it applies to this thesis. The chapter ends with a discussion on quadrature and an analysis of the resulting error.

2.1 Original formulation

As explained in the introduction, SPH uses a weighted integral and integration by parts to transfer derivatives over to the weighting, or shape, function. That is, given some function f defined on the interval $a \leq \xi \leq b$ we write the weighted, or smoothed, approximation of f at some point x as

$$< f > (x) = \int_a^b f(\xi)\, W(\xi - x, r)\, d\xi \tag{2.1}$$

where W is the shape function and r is its width, that is, the extent of its support. Here we write W as a function of $\xi - x$ so that we can use the same W for every x. Using integration by parts we can, as before, write

$$< f' > (x) = - \int_a^b f(\xi)\, W'(\xi - x, r)\, d\xi \tag{2.2}$$

and

$$< f'' > (x) = \int_a^b f(\xi)\, W''(\xi - x, r)\, d\xi \tag{2.3}$$

so long as $W(a - x, r) = W(b - x, r) = 0$ and $W'(a - x, r) = W'(b - x, r) = 0$. Now all we have to do is ensure that $< f > \rightarrow f$ as $r \rightarrow 0$. In the SPH literature this is done by stipulating that W must converge to the Dirac delta as $r \rightarrow 0$, in some sense (see Figure 2.1). In the limit as $r \rightarrow 0$, equation (2.1) would become the Dirac identity, for which

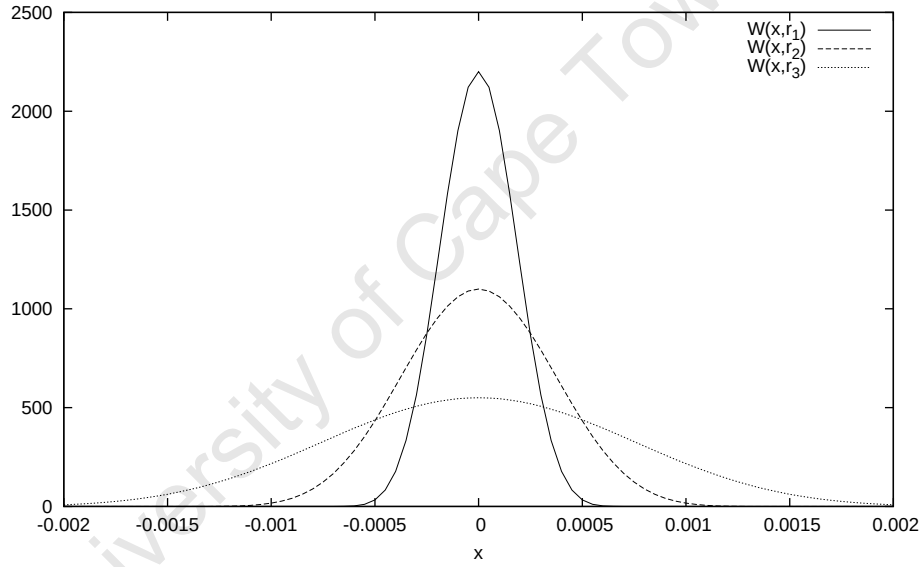

FIGURE 2.1: Shape function $W(x, r)$ for $r_1 < r_2 < r_3$

the sampling property

$$f(x) = \int_{-\infty}^{\infty} f(\xi)\, \delta(\xi - x)\; d\xi \tag{2.4}$$

is exact. That is, W is a delta sequence[1]. In order to satisfy this property the shape function W is stipulated to have the following properties:

[1] According to Weisstein [7] the Dirac delta function can be defined as the limit of a delta sequence :

$$\lim_{n \rightarrow \infty} \int_{\infty}^{\infty} \delta_n(x - a) f(x)\; dx = f(a)$$

In other words, δ_n is a sequence of functions such that as $n \rightarrow \infty$ the integral $\rightarrow f(a)$. So W is a delta sequence with $r_n \rightarrow 0$ as $n \rightarrow \infty$.

(i) the function is positive; that is,

$$W(x,r) \;\geq\; 0 \quad \forall\, x \quad ; \tag{2.5}$$

(ii) the function is even; that is,

$$W(-x,r) \;=\; W(x,r) \quad \forall\, x \quad ; \tag{2.6}$$

(iii) the area under the function is unity; that is,

$$\int_{-\infty}^{\infty} W(x,r)\; dx \;=\; 1 \quad ; \tag{2.7}$$

and (iv) W has compact support; that is,

$$W(x,r) = 0 \quad \text{for } |x| > r \quad . \tag{2.8}$$

It is also common knowledge that the shape function must be C^n continuous, where n is the highest derivative one wishes to calculate. This is because this requires the n^{th} derivative of W.

The shape functions most often used are either polynomial or exponential functions. A common choice is a spline. Possibly the most frequently utilised is the cubic B-spline (see Figure 2.2),

$$W(q,r) = \frac{4}{3r}\begin{cases} 1 - \frac{3}{2}q^2 + \frac{3}{4}q^3 & \text{if } 0 \leq q \leq 1 \\ \frac{1}{4}(2-q)^3 & \text{if } 1 \leq q \leq 2 \\ 0 & \text{if } q \geq 2 \end{cases} \tag{2.9}$$

where $q = 2|\xi - x|/r$. It is, as the name suggests, third-order continuous. This makes it a candidate for approximating derivatives up to $f^{(3)}$. It satisfies all the requirements mentioned earlier. That is, it is positive, even, has an area of unity, and has compact support.

Another common choice is the gaussian (see Figure 2.3),

$$W(q,r) = \frac{2}{r\sqrt{\pi}}\, e^{-(q/r)^2} \tag{2.10}$$

where $q = 2|\xi - x|$. It is infinitely differentiable which makes it a good candidate for calculating higher-order derivatives. It is positive, even and has an area of unity. However, it should be noted that this function has infinite support, in contradiction to the shape function requirements. In most cases researchers have chosen to have "near compact" support by choosing a support radius "large enough" so that the function is

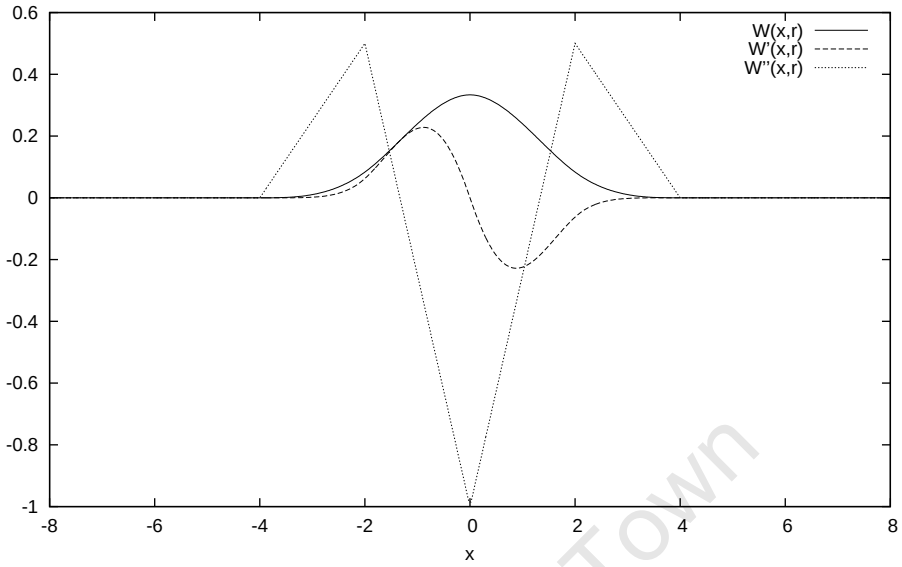

FIGURE 2.2: Cubic B-spline shape function and its derivatives

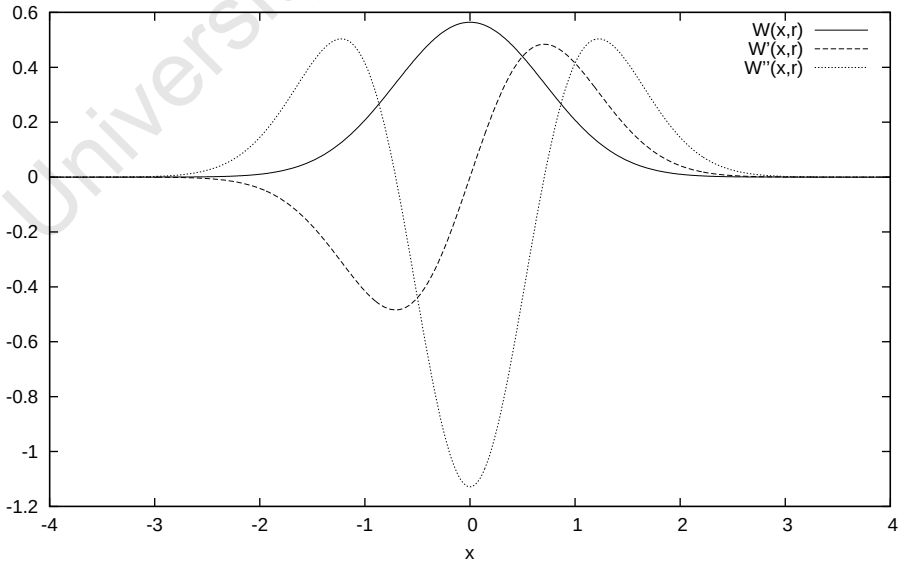

FIGURE 2.3: Gaussian shape function and its derivatives

sufficiently close to zero at the boundary. What effect this has on consistency is not clear. Also, the function is designed to have an area of unity below its entire support. Thus by cutting off the ends of the function in order to approximate it having zero at the boundaries also affects another requirement on the shape function. Again, what effect this has on consistency is not clear, and is not dealt with in this thesis.

In our tests we use a quintic spline (see Figure 2.4) which is defined by

$$W(q,r) = \frac{1}{30r}\begin{cases} (3-q)^5 - 6(2-q)^5 + 15(1-q)^5 & \text{if } 0 \le q \le 1 \\ (3-q)^5 - 6(2-q)^5 & \text{if } 1 \le q \le 2 \\ (3-q)^5 & \text{if } 2 < q \le 3 \\ 0 & \text{if } q > 3 \end{cases} \tag{2.11}$$

where $q = 4|\xi - x|/r$. It is fifth-order continuous and satisfies all the shape function

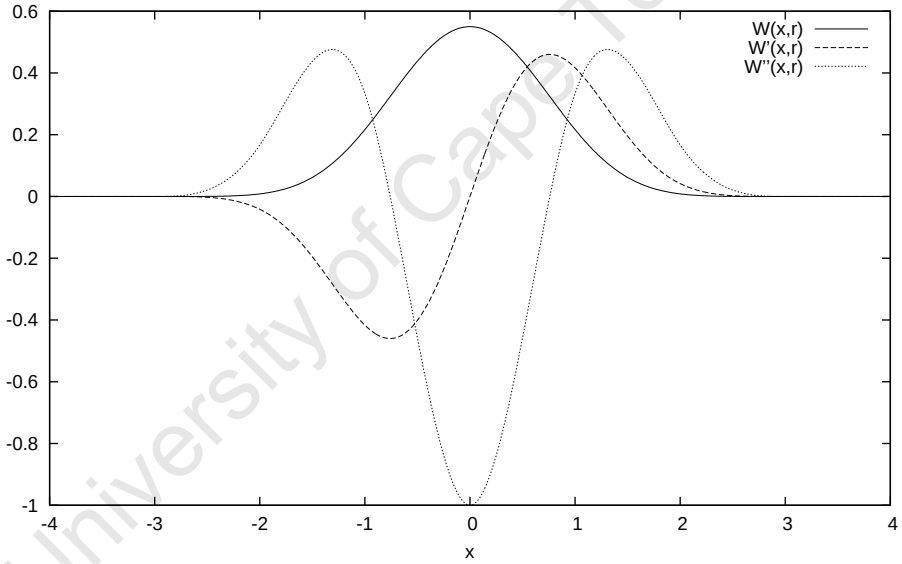

FIGURE 2.4: Quintic spline shape function and its derivatives

requirements mentioned earlier.

2.2 Consistency of weighted integrals

We now show under which conditions weighted approximations converge consistently as the support of the shape functions tend to zero. We do so without making any assumptions about the shape functions used. The function to be approximated is denoted by f and is assumed to be bounded and sufficiently smooth so that the required number of derivatives used in the derivations exist.

Let us define a function $F : \mathbb{R} \to \mathbb{R}$ with value at any point x in its domain equal to the integral of the product of f with a function g, which for the moment is arbitrary, and the support of which is the interval $x - r \leq \xi \leq x + r$. That is,

$$F(x) = \int_{x-r}^{x+r} f(\xi)g(\xi)\ d\xi \quad . \tag{2.12}$$

We now replace $f(\xi)$ with its Taylor expansion about the point x, so that

$$F(x) = \int_{x-r}^{x+r} \Big[f(x) + f'(x)(\xi - x) + f''(x)\frac{(\xi - x)^2}{2} + \ldots \Big] g(\xi)\ d\xi \tag{2.13}$$

where $f'(x) \equiv df(x)/d\xi$, $f''(x) \equiv d^2 f(x)/d\xi^2$, etc. Since $f(x)$, $f'(x)$, etc, are constants, we can rewrite (2.13) as

$$\begin{aligned} F(x) &= f(x) \int_{x-r}^{x+r} g(\xi)\ d\xi \\ &+ f'(x) \int_{x-r}^{x+r} (\xi - x)g(\xi)\ d\xi \\ &+ f''(x) \int_{x-r}^{x+r} \frac{(\xi - x)^2}{2} g(\xi)\ d\xi \\ &+ \ldots \end{aligned} \tag{2.14}$$

We now ask the question: under what conditions will $F(x) \to f(x)$ as $r \to 0$? Similarly, under what conditions will $F(x) \to f'(x)$ as $r \to 0$? And finally, under what conditions will $F(x) \to f''(x)$ as $r \to 0$?

Consider the case when

$$\int_{x-r}^{x+r} g(\xi)\ d\xi = 1 \tag{2.15}$$

which results in (2.14) becoming

$$\begin{aligned} F(x) &= f(x) \\ &+ f'(x) \int_{x-r}^{x+r} (\xi - x)g(\xi)\ d\xi \\ &+ f''(x) \int_{x-r}^{x+r} \frac{(\xi - x)^2}{2} g(\xi)\ d\xi \\ &+ \ldots \end{aligned} \tag{2.16}$$

Now noting that

$$\begin{aligned} \int_{x-r}^{x+r} (\xi - x)g(\xi)\ d\xi &\leq 2r \cdot \max|(\xi - x)| \cdot \max|g(\xi)| \\ &\leq 2r^2 \cdot \max|g(\xi)| \end{aligned}$$

we can see that the second term on the right hand side of (2.16) will approach zero as $r \to 0$ provided that

$$g(\xi) = O(r^k) \ , \quad k \geq -1 \quad . \tag{2.17}$$

Similarly for the higher-order terms, since

$$\begin{aligned} \int_{x-r}^{x+r} \frac{(\xi - x)^n}{n!} g(\xi) d\xi &\leq \frac{2r}{n!} \cdot \max |(\xi - x)^n| \cdot \max |g(\xi)| \\ &\leq 2r \cdot \frac{r^n}{n!} \cdot Cr^k \\ &\leq \frac{2Cr^{n+k+1}}{n!} \\ &\to 0 \quad \text{as } r \to 0 \quad \text{for } n = 1, 2, ... \quad \text{when } k \geq -1 \quad . \end{aligned}$$

Thus we can show that, under the conditions (2.15) and (2.17),

$$\int_{x-r}^{x+r} f(x) g(\xi) \ d\xi \ \to \ f(x) \ \text{ as } \ r \to 0 \quad . \tag{2.18}$$

We denote a function that satifies these constraints as g_0.

We can use a similar approach to ascertain when $F(x) \to f'(x)$ as $r \to 0$. We start by assuming now that g satisfies

$$\int_{x-r}^{x+r} g(\xi) \ d\xi \ = \ 0 \tag{2.19}$$

and

$$\int_{x-r}^{x+r} (\xi - x) g(\xi) \ d\xi \ = \ 1 \quad . \tag{2.20}$$

Then (2.14) becomes

$$\begin{aligned} F(x) &= f'(x) \\ &+ f''(x) \int_{x-r}^{x+r} \frac{(\xi - x)^2}{2} g(\xi) \ d\xi \\ &+ \ \ldots \end{aligned} \tag{2.21}$$

Noting that

$$\begin{aligned} \int_{x-r}^{x+r} \frac{(\xi - x)^2}{2} g(\xi) \ d\xi &\leq r \cdot \max |(\xi - x)^2| \cdot \max |g(\xi)| \\ &\leq r^3 \cdot \max |g(\xi)| \end{aligned}$$

we can see that the second term on the right hand side of (2.21) will approach zero as $r \to 0$ provided that

$$g(\xi) = O(r^k) \ , \quad k \geq -2 \quad . \tag{2.22}$$

Similarly for the higher-order terms, as before. Thus we can show that under the conditions (2.19), (2.20) and (2.22)

$$\int_{x-r}^{x+r} f(\xi)g(\xi)\ d\xi \ \rightarrow\ f'(x) \ \text{ as } \ r \rightarrow 0 \quad . \tag{2.23}$$

We denote a function that satisfies these constraints as g_1.

Finally, to find a function g which ensures that $F(x) \rightarrow f''(x)$ as $r \rightarrow 0$ we first ensure that

$$\int_{x-r}^{x+r} g(\xi)\ d\xi \ = \ 0 \quad , \tag{2.24}$$

$$\int_{x-r}^{x+r} (\xi - x)g(\xi)\ d\xi \ = \ 0 \quad , \tag{2.25}$$

and

$$\int_{x-r}^{x+r} \frac{(\xi - x)^2}{2} g(\xi)\ d\xi \ = \ 1 \quad . \tag{2.26}$$

Then (2.14) becomes

$$\begin{aligned} F(x) \ &= \ f''(x) \\ &+ \ f'''(x) \int_{x-r}^{x+r} \frac{(\xi - x)^3}{3!} g(\xi)\ d\xi \\ &+ \ \ldots \end{aligned}$$

and as before we can show that this will approach zero as $r \rightarrow 0$ provided that

$$g(\xi) = O(r^k)\ , \quad k \geq -3 \quad . \tag{2.27}$$

We can thus show that under the conditions (2.24), (2.25) and (2.27)

$$\int_{x-r}^{x+r} f(\xi)g(\xi)\ d\xi \ \rightarrow\ f''(x) \ \text{ as } \ r \rightarrow 0 \quad . \tag{2.28}$$

We denote a function that satisfies these conditions by g_2.

In Section 2.4 we provide examples of g_0, g_1 and g_2 which satisfy the minimum constraints on order, i.e. $g_0(\xi) = O(1/r)$, $g_1(\xi) = O(1/r^2)$, and $g_2(\xi) = O(1/r^3)$. Monaghan [31] shows that the smoothing error, e_s, defined by

$$e_s(x) = \Big| f(x) - < f > (x) \Big| \quad , \tag{2.29}$$

satisfies $e_s(x) = O(r^k)$ where k is dependent on the shape function. From (2.17), (2.22) and (2.27) we see that the smoothing error under these minimal constraints is $e_s(x) = O(r)$.

2.3 Consistency of standard shape functions

In this section we investigate whether the shape function conditions presented in Section 2.1 imply the consistency conditions developed in Section 2.2.

Let us denote by W any shape function which satisfies the conditions in Section 2.1 with W' and W'' its first and second derivatives, respectively, and for brevity's sake let us assume all integrals in this section are between $x - r$ and $x + r$. Consider first the conditions defining g_0. The fact that

$$\int W \, d\xi \;=\; 1 \tag{2.30}$$

means that W satisfies the conditions for g_0 so long as $W = O(r^k)$, $k \geq -1$. Since W is even that means that W' is odd. This implies that

$$\int W' \, d\xi \;=\; 0 \tag{2.31}$$

which satisfies the first condition (2.19) for g_1. The second condition (2.20) becomes

$$\begin{aligned} \int (\xi - x)\, W' \, d\xi \quad &= \int \xi \, W' \; d\xi \;-\; x \int W' \; d\xi \\ &= \int \xi \, W' \; d\xi \;-\; x \Big[W \Big]_{x-r}^{x+r} \\ &= \int \xi \, W' \; d\xi \end{aligned} \tag{2.32}$$

since W has compact support. Now using integration by parts (2.32) becomes

$$\int (\xi - x)\, W' \, d\xi \quad = \int \xi \, W' \, d\xi \tag{2.33}$$

$$= \Big[\xi W \Big]_{x-r}^{x+r} - \int W \, d\xi \tag{2.34}$$

$$= -1 \tag{2.35}$$

since the integral of W is stipulated to be unity. The moment is negative but since in standard SPH we set

$$< f' > = - \int W' f \; d\xi \quad , \tag{2.36}$$

W' is a candidate for g_1, so long as $W' = O(r^k)$, $k \geq -2$.

Finally, consider the conditions for g_2. We have

$$\int \frac{(\xi - x)^2}{2} W'' \, d\xi = \; \frac{1}{2} \int \xi^2 \, W'' \, d\xi \;-\; x \int \xi \, W'' \, d\xi \;+\; \frac{x^2}{2} \int W'' \, d\xi \tag{2.37}$$

which, using integration by parts, becomes

$$\begin{aligned}\int \frac{(\xi - x)^2}{2} W'' \, d\xi &= \frac{1}{2}\Big[\xi^2 W'\Big]_{x-r}^{x+r} - \int \xi W' \, d\xi \\ &\quad - x\Big[\xi W'\Big]_{x-r}^{x+r} + x\int W' \, d\xi \\ &\quad + \frac{x^2}{2}\Big[W'\Big]_{x-r}^{x+r} \quad .\end{aligned}$$

Performing integration by parts again on the second term on the right hand side, this becomes

$$\begin{aligned}\int \frac{(\xi - x)^2}{2} W'' \, d\xi &= \frac{1}{2}\Big[\xi^2 W'\Big]_{x-r}^{x+r} - \Big[\xi W\Big]_{x-r}^{x+r} + \int W \, d\xi \\ &\quad - x\Big[\xi W'\Big]_{x-r}^{x+r} + x\Big[W\Big]_{x-r}^{x+r} \\ &\quad + \frac{x^2}{2}\Big[W'\Big]_{x-r}^{x+r}\end{aligned}$$

which equals unity so long as W' is zero at the boundary. There is no such explicit requirement; however, such a requirement is implied when developing the approximation to the second gradient. That is, to arrive at

$$< f'' > (x) = \int f(\xi)\, W''(\xi - x, r)\, d\xi \tag{2.38}$$

one performs integration by parts twice, such that

$$< f'' > (x) = \int f''(\xi)\, W(\xi - x, r)\, d\xi \tag{2.39}$$

$$= \Big[f'(\xi)\, W(\xi - x, r) \Big]_{x-r}^{x+r} - \int f'(\xi)\, W'(\xi - x, r)\, d\xi \tag{2.40}$$

$$= 0 - \Big[f(\xi)\, W'(\xi - x, r) \Big]_{x-r}^{x+r} + \int f(\xi)\, W''(\xi - x, r)\, d\xi \tag{2.41}$$

$$= \int f(\xi)\, W''(\xi - x, r)\, d\xi \tag{2.42}$$

provided that W' is zero at $\xi = x \pm r$. This step is never made clear in the SPH literature but it is a necessary requirement. In fact, in order to follow this procedure for higher gradients one requires higher order derivatives to be zero at the extremities, so that in order to approximate f^n we require that

$$W^k\Big|_{x-r}^{x+r} = 0 \quad \text{for} \quad k = 0, 1, 2...n-1 \quad . \tag{2.43}$$

In any case, both these constraints and the constraints on order are met by the quintic and the B-spline shape functions, which are used in this thesis.

Thus the SPH shape function conditions are not sufficient to ensure consistency and

convergence. In addition to the conditions described, they need to ensure (2.43), which are implied in the SPH equation derivations, and also that W is of order r^k, $k \geq -1$. Both of these conditions are met, however, when using shape functions common in the SPH literature such as the cubic or the B-splines.

2.4 Piecewise-linear consistent shape functions

What are the simplest shape functions which satisfy the constraints in Section 2.2? For g_0 we can satisfy

$$\int_{x-r}^{x+r} g_0(\xi)\, d\xi \;=\; 1 \tag{2.44}$$

with a constant function,

$$g_0(\xi) = \frac{1}{2r} \quad , \tag{2.45}$$

which is of order $1/r$, the minimum constraint required. Applying this to our smoothed approximation we arrive at

$$<f>(x) = \frac{1}{2r}\int_{x-r}^{x+r} f(\xi)\, d\xi \quad . \tag{2.46}$$

Thus g_0 generates a smoothed approximation $<f>$ which is simply the average value of f.

For g_1 we can use a linear function

$$g_1(\xi) = \frac{3}{2r^3}\,(\xi - x) \tag{2.47}$$

which satisfies

$$\int_{x-r}^{x+r} g_1(\xi)\, d\xi \;=\; 0 \tag{2.48}$$

since it is odd about $\xi = x$, and

$$\int_{x-r}^{x+r} (\xi - x)\, g_1(\xi)\, d\xi \;=\; 1 \quad , \tag{2.49}$$

and is of order $1/r^2$, again the minimum constraint.

Finally for g_2 we can use a piecewise-linear function

$$g_2(\xi) = \frac{6}{r^4}\Big[2|\xi - x| - r\Big] \tag{2.50}$$

which satisfies

$$\int_{x-r}^{x+r} g_2(\xi)\, d\xi \;=\; 0 \quad , \tag{2.51}$$

$$\int_{x-r}^{x+r} (\xi - x)\ g_2(\xi)\ d\xi \ = \ 0 \quad , \tag{2.52}$$

and

$$\int_{x-r}^{x+r} \frac{(\xi - x)^2}{2}\ g_2(\xi)\ d\xi \ = \ 1 \quad , \tag{2.53}$$

and is of order $1/r^3$, also the minimum constraint.

Thus these three shape functions satisfy the minimum constraints on functions which ensure that

$$\int_{x-r}^{x+r} f(\xi) g_0(\xi) d\xi \ \rightarrow \ f(x) \quad \text{as } r \rightarrow 0 \quad , \tag{2.54}$$

$$\int_{x-r}^{x+r} f(\xi) g_1(\xi) d\xi \ \rightarrow \ f'(x) \quad \text{as } r \rightarrow 0 \quad , \tag{2.55}$$

and

$$\int_{x-r}^{x+r} f(\xi) g_2(\xi) d\xi \ \rightarrow \ f''(x) \quad \text{as } r \rightarrow 0 \quad . \tag{2.56}$$

See Figure 2.5 for plots of these shape functions when $r = 4$.

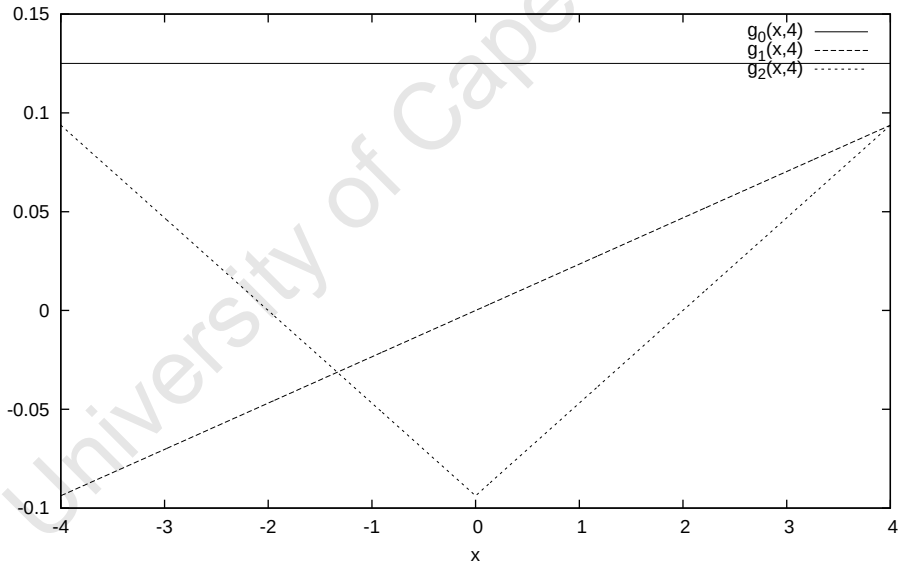

FIGURE 2.5: Consistent linear shape functions for $r = 4$

Thus in contrast to the conventional approach, different kernels are used in the interpolation of functions and their various derivatives.

As mentioned in Section 2.2, the minimal smoothing error for a general function g_n is $e_s = O(r)$. However, the specific choices of $g_n (n = 0, 1, 2)$ in (2.44), (2.47) and (2.50) are respectively even, odd, and even, so that the leading term in the error is one order higher. Thus for these functions

$$e_s = O(r^2) \quad . \tag{2.57}$$

2.5 Domain extension

SPH originally was used to model scattered masses in outer space. This meant that the effects of the smoothing approximations at the edges of the domain could be deemed negligible. This is not the case in our situation, however, where the domain is bounded. When the point x is sufficiently close to one of the boundaries so that the support of the shape function is not contained within the interval $[a, b]$, the approximations in the previous section are no longer valid. This is because all the derivations used assumed that the full support of the shape functions were being integrated. Therefore when approximating a function over a bounded domain it is necessary to modify the approximation in such a way as to accommodate these constraints. One technique used is to replace f with a new function $\tilde{f}$ defined as the smooth extension of f on the domain $[-r+a, b+r]$, smooth meaning that $\tilde{f}$ possesses sufficient derivatives at the boundaries. In order to understand what this implies for our consistency conditions, we place $\tilde{f}$ into our formulation in Section 2.2, equation (2.12); that is,

$$F(x) = \int_{x-r}^{x+r} \tilde{f}(\xi) g(\xi)\, d\xi \quad . \tag{2.58}$$

We now replace $\tilde{f}(\xi)$ with its Taylor expansion about the point x, so that

$$F(x) = \int_{x-r}^{x+r} \Big[\tilde{f}(x) + \tilde{f}'(x)(\xi - x) + \tilde{f}''(x)\frac{(\xi - x)^2}{2} + \ldots\Big] g(\xi)\, d\xi \quad . \tag{2.59}$$

As before, we can use (2.59) to deduce when $g(\xi)$ will allow for consistent approximations for $<f>$, $<f'>$, etc. However, (2.59) requires that $\tilde{f}'(x)$, $\tilde{f}''(x)$, etc. exist. Therefore the domain extension must ensure continuity at the boundary for every gradient up to the gradient which is being approximated. So when calculating $<f'>$ we must ensure that $\tilde{f}$ is continuously differentiable. When calculating $<f''>$ we must ensure that $\tilde{f}$ is twice continuously differentiable.

One common technique used in this regard in the SPH literature is called *ghost particles* (first introduced in [21]) which simply extends f with a function of constant value set to the value at the boundaries. Thus zero order consistency is ensured. This would only allow for consistent approximations for $<f>$, as one would expect. Another approach is that of Schwaiger [8] in which f is extended beyond the boundary in such a way that $f(x) - f(a)$ is odd about the boundary $x = a$. This ensures continuity of the first derivative and is thus sufficient to produce consistent approximations for $<f>$ and $<f'>$.

In this thesis we will use Lagrange polynomials to interpolate f to sufficient degree in extending it beyond the boundary. This allows for the consistent approximations of any

order. In Chapter 4 we show how this is implemented both for approximating functions and for solving the advection-diffusion equation.

2.6 Imposing boundary conditions

In SPH approximations of boundary value problems there is the issue of ensuring that boundary conditions are imposed. In virtually all of the SPH literature simulations are time-dependent and the algorithms are based on calculating the SPH approximations to derivatives in the current time step to work out the change needed to advance to the next time step. Boundary conditions thus need to be imposed on the SPH approximations themselves, i.e. values of $<f>$, $<f'>$, etc. need to approach the correct values at the boundaries. A general technique for imposing any boundary condition in such a situation has not yet been developed. However, in order to impose essential boundary conditions one can use a variation of the ghost particle method mentioned in the previous section. By extending f correctly one can ensure that $<f>$ approaches any desired value at the boundary. For an example of how this is done see [6]. In this thesis we will solve the steady advection-diffusion equation. Thus we can impose the conditions directly. For more on how this is done see Section 4.4.

2.7 Numerical integration

In order to evaluate $<f>$, $<f'>$ and $<f''>$ one must use a quadrature technique to approximate the integrals numerically. This introduces a further source of error into the problem. For example, $\widehat{<f>}(x)$ is defined to be the discrete approximation of the smoothed approximation $<f>$ of f, obtained by integrating using a quadrature rule. We write the discretisation error as

$$e_d(x) = |\, <f>(x) - \widehat{<f>}(x)| \quad . \tag{2.60}$$

Using the rectangular rule and evenly spaced particles this becomes

$$e_d(x) = \Big| \int_{x-r}^{x+r} f(\xi) W(\xi - x, r)\, d\xi \; - \; \sum_j f(x_j) W(x_j - x, r) \Delta x \Big| \tag{2.61}$$

where Δx is the particle spacing.

We follow the approach of Quinlan et al. [20] in analysing the error. For this we need the Euler-Maclaurin formula:

$$\Delta x \sum_{j=1}^{N} \overline{f}_j = \int_{x_1-\Delta x/2}^{x_N+\Delta x/2} \overline{f}(\xi)\, d\xi + \sum_{k=1}^{\infty} C_k \Delta x^{2k} \left[\overline{f}^{(2k-1)}\right]_{x_{1/2}}^{x_{N+1/2}} \tag{2.62}$$

for a function $\overline{f}$, in which the constants C_k decrease as $k \to \infty$. Here N is the number of nodes on the domain $a \leq x \leq b$, i.e. $\Delta x = (b-a)/(N-1)$, and $x_i = a + (i-1)\Delta x$, $i = 1, 2, ...N$.

Choose $\overline{f} = f\, g_n$: then the left hand side of (2.62) is $\widehat{\langle f^{(n)} \rangle}$, the discretized SPH approximation of $f^{(n)}$, and the first term on the right hand side is $\langle f^{(n)} \rangle$. Technically the first term on the right hand side is

$$\langle f^{(n)} \rangle + \int_{-\Delta x/2}^{0} \overline{f}(\xi)\, d\xi \; + \; \int_{0}^{\Delta x/2} \overline{f}(\xi)\, d\xi \quad . \tag{2.63}$$

However, these two integrals both approach zero as $\Delta x \to 0$. We therefore omit them for convenience.

It follows that

$$\left| \langle f^{(n)} \rangle - \widehat{\langle f^{(n)} \rangle} \right| = \left| \sum_{k=1}^{\infty} \underbrace{C_k \Delta x^{2k} \left[\overline{f}^{(2k-1)}\right]_{x_{1/2}}^{x_{N+1/2}}}_{\text{call this } E_k} \right| \quad . \tag{2.64}$$

The total error at any point x is estimated as follows:

$$\begin{aligned} \text{Total error } \left| f - \widehat{\langle f^{(n)} \rangle} \right| &= \left| f - \langle f^{(n)} \rangle + \langle f^{(n)} \rangle - \widehat{\langle f^{(n)} \rangle} \right| \\ &\leq \underbrace{\left| f - \langle f^{(n)} \rangle \right|}_{\text{smoothing error}} + \underbrace{\left| \langle f^{(n)} \rangle - \widehat{\langle f^{(n)} \rangle} \right|}_{\text{discretization error}} . \end{aligned} \tag{2.65}$$

The first term on the right hand side of (2.65) is dependent on the shape function used and is of order r^n, $n \geq 1$ (see (2.57) and [6] and [20] for more on this). The next task is to estimate the second term on the right hand side, using (2.64). We do this for the first and second derivative, i.e. for $n = 1$ and $n = 2$.

The case $n = 1$

We want to estimate the discretisation error in the first derivative. For convenience, consider the domain $[-r, r]$, so that $x_1 = -r$ and $x_N = r$. It follows that $x_{1/2} = -(r + \Delta x/2)$ and $x_{N+1/2} = r + \Delta x/2$.

Now consider the expression E_1 (see (2.64)) and expand in a Taylor series about $x = 0$: for $k = 1$,

$$\begin{aligned}\left[(fg_1)^{(1)}\right]_{x_{1/2}}^{x_{N+1/2}} &= \left[(fg_1)^{(1)}\right]_{-(r+\Delta x/2)}^{r+\Delta x/2} \\ &= \left[(fg_1)_0^{(1)} + (fg_1)_0^{(2)}(r + \Delta x/2) + \text{h.o.t.}\right] \\ &\quad - \left[(fg_1)_0^{(1)} - (fg_1)_0^{(2)}(r + \Delta x/2) + \text{h.o.t.}\right] .\end{aligned}$$

It follows that

$$\left[(fg_1)^{(1)}\right]_{x_{1/2}}^{x_{N+1/2}} = 2\,(fg_1)_0^{(2)}\,(r + \Delta x/2) + \text{h.o.t.} \quad . \tag{2.66}$$

Now take a closer look at the term $(fg_1)_0^{(2)}$: bearing in mind that

$$g_1(\xi) = \frac{3\xi}{2r^3}\,, \tag{2.67}$$

$$\begin{aligned}(fg_1)_0^{(2)} &= \left[f''g_1 + 2f'g_1' + fg_1''\right]_{\xi=0} \\ &= 0 + \frac{3}{r^3}f_0' + 0\,.\end{aligned}$$

Thus, from (2.64) the first term on the right hand side of (2.64) is

$$\begin{aligned}E_1 &= \frac{3C_1}{r^3}f_0' \cdot (r + \Delta x/2) \cdot (\Delta x)^2 + \text{h.o.t.} \\ &= 3C_1 f_0' \left(\frac{\Delta x}{r}\right)^2 + \text{h.o.t.}\,.\end{aligned} \tag{2.68}$$

Next, consider the term $k = 2$, ie.

$$\begin{aligned}E_2 &= C_2(\Delta x)^4 \left[(fg_1)^{(2)}\right]_{-(r+\Delta x/2)}^{r+\Delta x/2} \\ &= 2\,C_2(\Delta x)^4 (fg_1)_0^{(3)}(r + \Delta x/2) + \text{h.o.t.}\end{aligned} \tag{2.69}$$

using a Taylor series expansion as before. Now

$$\begin{aligned}(fg_1)_0^{(3)} &= \left[f'''g_1 + 3f''g_1' + 3f'g_1'' + fg'''\right]_0 \\ &= 0 + \frac{9f_0''}{r^3} + 0 + 0\end{aligned}$$

so that, returning to (2.69),

$$\begin{aligned}E_2 &= 2\,C_2(\Delta x)^4(r + \Delta x/2)\frac{9f_0''}{r^3} + \text{h.o.t.} \\ &= 18f_0''r^2\left(\frac{\Delta x}{r}\right)^4 + \text{h.o.t.}\end{aligned} \tag{2.70}$$

which is of higher order than E_1.

Likewise, E_3, $E_4, \ldots$ will yield higher-order terms.

In conclusion, we find that the discretization error is given by

$$\left|\langle f^{(1)}\rangle - \widehat{\langle f^{(1)}\rangle}\right| = C\,f_0'\left(\frac{\Delta x}{r}\right)^2 + \text{h.o.t.}\,. \tag{2.71}$$

The case $n = 2$

Here we need

$$g_2(\xi) = \frac{6}{r^4}[2|\xi| - r]\,. \tag{2.72}$$

Since g_2 is piecewise-linear we write the integral in two parts, ie.

$$\begin{aligned}\langle f^{(2)}\rangle &= \int_{-r}^{r} f g_2\; d\xi \\ &= \underbrace{\int_{-r}^{0} f g_2\; d\xi}_{I_\ell} + \underbrace{\int_{0}^{r} f g_2\; dx}_{I_r}\,.\end{aligned} \tag{2.73}$$

Start with I_r: from (2.62), and assuming that N is odd, we have

$$\Delta x \sum_{(N+1)/2}^{N} \overline{f}_j = \int_{x_{(N+1)/2}-\Delta x/2}^{x_N+\Delta x/2} \overline{f}(\xi)\; d\xi + \sum_{k=1}^{\infty} C_k \Delta x^{2k}\left[\overline{f}^{(2k-1)}\right]_{x_{(N+1)/2}-\Delta x/2}^{x_N+\Delta x/2} \tag{2.74}$$

bearing in mind that we have the same partitioning as before, and the range for I_r is $[x_{(N+1)/2}, x_N]$ when N is odd. The case of even N can be treated in a similar way and is omitted.

Proceed as before, and take the terms corresponding to $k = 1$, then expand in a Taylor series about $x_{mid} = \frac{1}{2}(x_{(N+1)/2} + x_N) = r/2$:

$$\begin{aligned}
\Big[(fg_2)^{(1)}\Big]_{x_{(N+1)/2}-\frac{\Delta x}{2}}^{x_N+\frac{\Delta x}{2}} &= \Big[(fg_2)^{(1)}\Big]_{-\Delta x/2}^{r+\Delta x/2} \\
&= \Big[(fg_2)^{(1)}_{x_{mid}} + (fg_2)^{(2)}_{x_{mid}}\tfrac{1}{2}(r+\Delta x) + \text{hot}\Big] \\
&\quad - \Big[(fg_2)^{(1)}_{x_{mid}} - (fg_2)^{(2)}_{x_{mid}}\tfrac{1}{2}(r+\Delta x) + \text{hot}\Big] \\
&= 2\,(fg_2)^{(2)}_{x_{mid}}\tfrac{1}{2}(r+\Delta x) + \text{hot} \\
&= (f''g_2 + 2f'g_2' + fg_2'')_{x_{mid}}(r+\Delta x) + \text{hot} \\
&= [0 + \frac{24}{r^4}f'_{x_{mid}} + 0](r+\Delta x) + \text{hot}\,.
\end{aligned}$$

Thus

$$\begin{aligned}
E_{1r} &= C_1\,\frac{24}{r^4}\,f'_{x_{mid}}(r+\Delta x)(\Delta x)^2 + \text{h.o.t.} \\
&= 24C_1 f'_{x_{mid}}\Big[\Big(\frac{\Delta x}{r}\Big)^2\frac{1}{r} + \frac{1}{r}\Big(\frac{\Delta x}{r}\Big)^3\Big] \;+\; \text{h.o.t.}\,. \qquad (2.75)
\end{aligned}$$

Next, evaluate I_ℓ: again from (2.62), and assuming that N is odd,

$$\Delta x\sum_{j=1}^{(N+1)/2}(fg_2)_j = \int_{x_1-\Delta x/2}^{x_{(N+1)/2}+\Delta x/2} fg_2\,d\xi + \sum_{k=1}^{\infty}C_k\Delta x^{2k}\Big[(fg_2)^{(2k-1)}\Big]_{x_1-\Delta x/2}^{x_{(N+1)/2}+\Delta x/2}\,. \qquad (2.76)$$

Expanding in a Taylor series about $x_{mid} = \frac{1}{2}(x_1 + x_{(N+1)/2}) = -r/2$,

$$\begin{aligned}
\Big[(fg_2)^{(1)}\Big]_{x_1-\Delta x/2}^{x_{(N+1)/2}+\Delta x/2} &= \Big[(fg_2)^{(1)}\Big]_{-(r+\Delta x/2)}^{\Delta x/2} \\
&= \Big[(fg_2)^{(1)}_{x_{mid}} + (fg_2)^{(2)}_{x_{mid}}\tfrac{1}{2}(r+\Delta x) + \text{hot}\Big] \\
&\quad - \Big[(fg_2)^{(1)}_{x_{mid}} - (fg_2)^{(2)}_{x_{mid}}\tfrac{1}{2}(-(r+\Delta x)) + \text{hot}\Big] \\
&= (fg_2)^{(2)}_{x_{mid}}(r+\Delta x) + \text{hot} \\
&= (f''g_2 + 2f'g_2' + fg_2'')_{x_{mid}}(r+\Delta x) + \text{hot} \\
&= [0 - \frac{12}{r^4}f'_{x_{mid}} + 0](r+\Delta x) + \text{hot}
\end{aligned}$$

Hence

$$\begin{aligned}
E_1 &= E_{1\ell} + E_{1r} \\
&= 24\frac{1}{r}\,\Big[f'(\frac{r}{2}) - f'(-\frac{r}{2})\Big]\,\Big[\Big(\frac{\Delta x}{r}\Big)^2 + \Big(\frac{\Delta x}{r}\Big)^3 + \text{hot}\Big] \\
&= 24C_1 f''(0)\Big(\frac{\Delta x}{r}\Big)^2 + \text{hot} \qquad (2.77)
\end{aligned}$$

As for the case $n = 1$, it can be shown that the terms corresponding to $k = 2, 3, \ldots$ are of higher order.

In summary, we find that

$$\text{Discretization error } e_d = O\left(\frac{\Delta x}{r}\right)^2$$

as $(\Delta x/r) \to 0$ and $r \to 0$. Thus the total error e is given by

$$e = e_d + e_s = O(\left(\frac{\Delta x}{r}\right)^2 + r^2) \tag{2.78}$$

for the shape function g_2 defined earlier. This means that, as was found experimentally by Laguna [24] and analytically by Quinlan [20], the error will not converge as $r \to 0$ unless one also ensures that $(\Delta x/r)^2 \to 0$ as well.

Chapter 3

Advection-diffusion problems

In this chapter we develop the boundary value problem used to test SPH. We start with a derivation for the steady 1D advection-diffusion equation, follow by highlighting the characteristic Peclet number, and end with a presentation of the boundary value problem we used in our tests showing the two cases of the Peclet number we investigated.

3.1 The advection-diffusion equation

Advection-diffusion occurs when a substance is both moving and diffusing at the same time. Consider the one-dimensional case of some substance of concentration $u(x)$ moving with velocity $v(x)$ and diffusing at the rate $q(x)$ through a pipe with area $A(x)$. By using the conservation principle we can say that

$$(Avu)_x + (Aq)_x = (Avu)_{x+\Delta x} + (Aq)_{x+\Delta x} \tag{3.1}$$

where x and $x + \Delta x$ are the boundaries of a control volume. Dividing throughout by Δx and taking the limit $\Delta x \to 0$ we obtain

$$\frac{d(Avu)}{dx} + \frac{d(Aq)}{dx} = 0 \tag{3.2}$$

If the diffusion is linear then Fick's first law holds, so

$$q = -k\frac{du}{dx} \tag{3.3}$$

where k is the diffusivity. Assuming constant area and velocity and substituting (3.3) into (3.1) we get

$$v\frac{du}{dx} - k\frac{d^2u}{dx^2} = 0 \tag{3.4}$$

which is the steady 1D advection-diffusion equation.

3.2 The Peclet number

Suppose the problem is defined on the domain $0 \leq x \leq L$. To non-dimensionalise we set $\overline{x} = \frac{x}{L}$; then

$$\frac{d}{dx} = \frac{1}{L} \cdot \frac{d}{d\overline{x}} \tag{3.5}$$

and

$$\frac{d^2}{dx^2} = \frac{1}{L^2} \cdot \frac{d^2}{d\overline{x}^2} \quad . \tag{3.6}$$

Substituting into (3.4) we get

$$v\frac{du}{d\overline{x}} \cdot \frac{1}{L} - k\frac{d^2u}{d\overline{x}^2} \cdot \frac{1}{L^2} = 0 \quad . \tag{3.7}$$

Now, multiplying by L and dividing by v we arrive at

$$\frac{du}{d\overline{x}} - \frac{k}{vL} \cdot \frac{d^2u}{d\overline{x}^2} = 0 \quad . \tag{3.8}$$

We set

$$Pe = \frac{vL}{k} \quad ; \tag{3.9}$$

this is known as the Peclet number. It is the dimensionless parameter relating the rate of advection to the diffusion. Thus (3.8) becomes

$$u' - \frac{1}{Pe}u'' = 0 \tag{3.10}$$

where $u' \equiv \frac{du}{d\overline{x}}$, $u'' \equiv \frac{d^2u}{d\overline{x}^2}$.

3.3 Exact solutions

For the case in which the boundary conditions are

$$u(0) = 1 \quad , \tag{3.11}$$

$$u(1) = 0 \quad , \tag{3.12}$$

equation (3.10) has solution

$$u(x) = 1 - \frac{1 - e^{Pe(1-x)}}{1 - e^{Pe}} \quad . \tag{3.13}$$

When Pe is small (3.13) has a smooth, gradual solution (see solid line in Figure 3.1). When Pe is large (3.13) has a sharp boundary layer on its right side (see dotted line in Figure 3.1). These are the two solutions which we will be using to test our various SPH

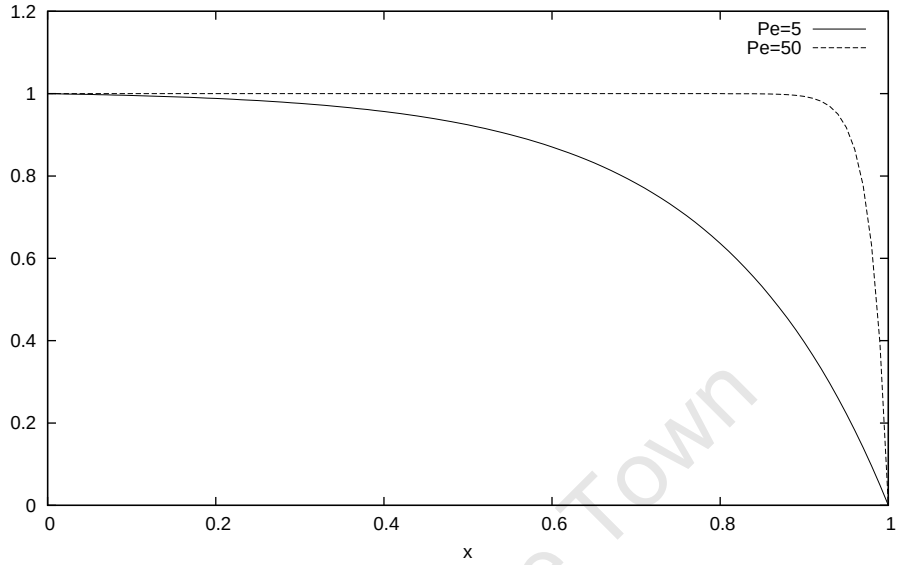

FIGURE 3.1: Equation (3.13) for different Peclet numbers

implementations, either by testing the production of gradients of the exact solutions or by trying to reproduce the solutions themselves by solving a system of linear equations, both using standard SPH and the new approach developed in Chapter 2.

When Pe is large (3.13) is said to be advection-dominated. Under these conditions piecewise-linear finite element approximations, which are equivalent to central difference approximations, lose accuracy (see Figure 3.2 and [12] for more). This has resulted in a lot of research to improve the situation with methods such as upwinding and SUPG (see, again, [12]). We felt that in light of these difficulties equation (3.10) would be a good problem to look at since we could test both an easy problem to solve using standard techniques (i.e. when Pe is low) and a hard problem to solve (i.e. when Pe is high).

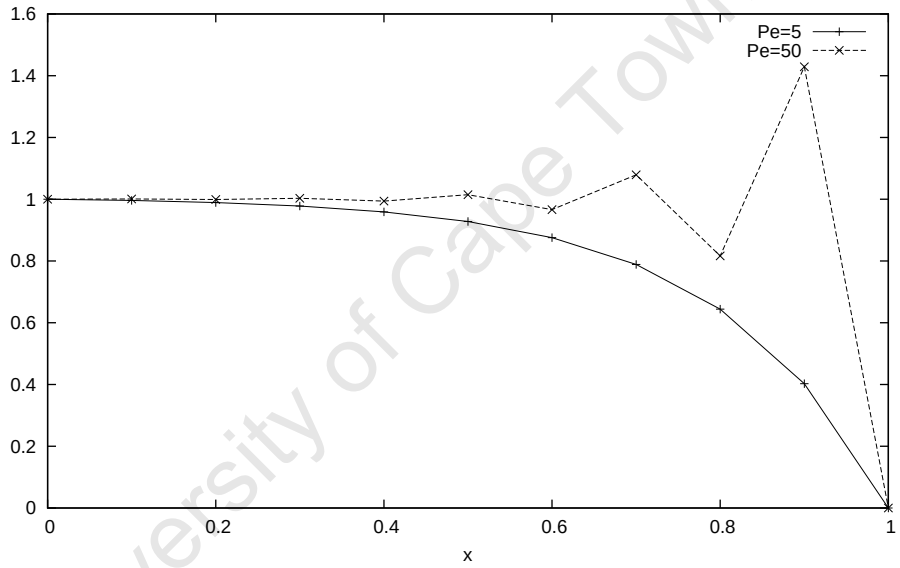

FIGURE 3.2: Finite element solution to Equation (3.10) for different Peclet numbers

Chapter 4

Results

In this chapter we present the results of the numerical experiments used to test the theory in Chapter 2. The first section explains how the domains were extended in order to ensure continuity at the boundary of any order. The next section details the various quadrature techniques employed. Next are the details of the methods and results on function and derivative approximation. Finally we present results on solutions to the advection-diffusion boundary value problem.

Unless otherwise stated all the tests in this chapter use the piecewise-linear shape functions described in Section 2.4 and use Simpson's rule for quadrature.

In order to ascertain the behaviour of the error with respect to the shape function support radius, r, a range of values of r is tested whilst holding $\Delta x/r$ constant. Unless otherwise stated, $\Delta x/r$ is set to 2/9, translating to four particles on either side of the shape function support.

4.1 Extending f

In Section 2.5 we show that in order to approximate f^n we need to ensure nth-order continuity at the boundary. To achieve this we used Lagrange polynomials to interpolate f to sufficient degree and used that interpolation to extend the function at either boundary.

In order to achieve nth-order continuity we need an approximation to f that is n-times continuously differentiable. Thus we approximate f in the neighbourhood of the boundary with an nth-order polynomial, using $n+1$ points of f. We take the n points of the discretised form of f adjacent to the boundary and use them to construct a nth-order polynomial. For example, the nth-order Lagrange polynomial used to extend f at

the left-hand boundary $x = a$ is $L(x)$,

$$L(x) = \sum_{j=0}^{n} f(x_j) l_j(x) \tag{4.1}$$

where $x_j \equiv a + j\Delta x$ and $l_j(x)$ are the Lagrange coefficients, defined by

$$l_j(x) = \prod_{i=0, i\neq j}^{n} \frac{x - x_i}{x_j - x_i} \quad . \tag{4.2}$$

We use a Lagrange polynomial to extend f at its boundaries to form $\bar{f}$. For example, given the function $f(x_i)$, $x_i = a + i\Delta x, i = 0, 1, 2...N-1$, in order to produce a two-point second-order extension on either side we write

$$\begin{aligned}
\bar{f}(x_i) &= \sum_{j=0}^{2} f(x_j) \prod_{k=0, k\neq j}^{2} \frac{x_i - x_k}{x_j - x_k} && i = -1, -2 \\
\bar{f}(x_i) &= f(x_i) && i = 0, ..., N-1 \\
\bar{f}(x_i) &= \sum_{j=N-3}^{N-1} f(x_j) \prod_{k=N-3, k\neq j}^{N-1} \frac{x_i - x_k}{x_j - x_k} && i = N, N+1
\end{aligned}$$

which produces a second-order polynomial on either side of the boundary by interpolating the three points in the domain and adjacent to the boundary.

4.2 Quadrature techniques

In Section 2.7 we discuss the error introduced through using the rectangular rule for quadrature. That is, in order to numerically approximate $<f^n>$ where

$$<f^n>(x) = \int f(\xi)\ g_n(\xi - x)\ d\xi \tag{4.3}$$

we write

$$\widehat{<f^n>}(x_i) = \sum_{j=0}^{k} f(x_j) g_n(x_j - x_i) \Delta x \tag{4.4}$$

where Δx is the particle spacing and k is the number of points used to integrate. In our tests we also consider the trapezoidal rule, defined by

$$\begin{aligned} \widehat{<f^{(n)}>}(x_i) &= \frac{f(x_0)g_n(x_0 - x_i)}{2} \\ &+ \sum_{j=1}^{k-1} f(x_j)g_n(x_j - x_i)\Delta x \\ &+ \frac{f(x_k)g_n(x_k - x_i)}{2} \end{aligned}$$

and Simpson's rule, defined by

$$\begin{aligned} \widehat{<f^{(n)}>}(x_i) &= \frac{f(x_0)g_n(x_0 - x_i)}{3} \\ &+ 2\sum_{j=1}^{k/2-1} f(x_j)g_n(x_j - x_i)\Delta x + \sum_{j=1}^{k/2} f(x_j)g_n(x_j - x_i)\Delta x \\ &+ \frac{f(x_k)g_n(x_k - x_i)}{3} \quad , \end{aligned}$$

where the fractions $k/2-1$ and $k/2$ specify that the sums are over odd and even values of j, respectively.

4.3 SPH approximations

In this section we look at SPH approximations to functions and their derivatives. That is, given an exact function f on a certain domain and its nth derivative $f^{(n)}$, what is the error of the SPH approximation to the nth derivative $\widehat{<f^{(n)}>}$?

We start by writing the smoothed approximation to the nth derivative of f at a point x, such that

$$<f^{(n)}>(x) = \int_{x-r}^{x+r} \tilde{f}(\xi)g_n(\xi - x)\, d\xi \tag{4.5}$$

where $\tilde{f}$ is the form of f extended to ensure sufficient continuity at the boundary (see previous section). Using the rectangle rule for quadrature, the discrete approximation can be written as

$$\widehat{<f^{(n)}>}(x) = \sum_{i=-n_r}^{n_r} \tilde{f}(x + i\Delta x)g_n((x + i\Delta x) - x)\ \Delta x \tag{4.6}$$

$$= \sum_{i=-n_r}^{n_r} \tilde{f}(x + x_i)g_n(i\Delta x)\ \Delta x \tag{4.7}$$

where Δx is the internodal spacing and n_r is the number of particles on either side of the support function.

To illustrate this, suppose that we are using six particles to discretise the domain $a \leq x \leq b$, five particles under the shape function cover and the rectangle rule for quadrature. We can write the discretised approximation to $f^{(n)}$ in vector form as

$$\begin{bmatrix} \widehat{<f^{(n)}>}(x_0) \\ \widehat{<f^{(n)}>}(x_1) \\ \widehat{<f^{(n)}>}(x_2) \\ \widehat{<f^{(n)}>}(x_3) \\ \widehat{<f^{(n)}>}(x_4) \\ \widehat{<f^{(n)}>}(x_5) \end{bmatrix} = \Delta x \begin{bmatrix} g_{-2} & g_{-1} & g_0 & g_1 & g_2 & \cdot & \cdot & \cdot & \cdot & \cdot \\ \cdot & g_{-2} & g_{-1} & g_0 & g_1 & g_2 & \cdot & \cdot & \cdot & \cdot \\ \cdot & \cdot & g_{-2} & g_{-1} & g_0 & g_1 & g_2 & \cdot & \cdot & \cdot \\ \cdot & \cdot & \cdot & g_{-2} & g_{-1} & g_0 & g_1 & g_2 & \cdot & \cdot \\ \cdot & \cdot & \cdot & \cdot & g_{-2} & g_{-1} & g_0 & g_1 & g_2 & \cdot \\ \cdot & \cdot & \cdot & \cdot & \cdot & g_{-2} & g_{-1} & g_0 & g_1 & g_2 \end{bmatrix} \begin{bmatrix} \bar{f}_a(x_{-2}) \\ \bar{f}_a(x_{-1}) \\ f(x_0) \\ f(x_1) \\ f(x_2) \\ f(x_3) \\ f(x_4) \\ f(x_5) \\ \bar{f}_b(x_6) \\ \bar{f}_b(x_7) \end{bmatrix}$$

where $x_i \equiv a + i\Delta x$, $g_i \equiv g_n(i\Delta x)$ is the shape function used to approximate the nth derivative and $\bar{f}_a$ and $\bar{f}_b$ are the Lagrange polynomials used to extend f at a and b, respectively. As can be seen, f is extended to ensure that the full support of g_n is included when centered at the boundaries.

Once we have calculated the discrete approximation to $f^{(n)}$ we then calculate the maximum relative error as

$$e_{max} = \frac{\max_j |f^{(n)}(x_j) - \widehat{<f^{(n)}>}(x_j)|}{\max_j |f^{(n)}(x_j)|} \quad , \tag{4.8}$$

where $\max_j$ is the maximum over all nodes j. As mentioned in Section 2.7, $e = e_d + e_s$ where e_d is of order $(\Delta x/r)^2$ and e_s is of order r^k, $k \geq 1$, and for the functions g $e_s = O(r^2)$ (see Section 2.4 for more).

4.3.1 Test functions

Three functions are used as examples in assessing the accuracy of approximations. These are, first, the solutions to the advection-diffusion equation described in Chapter 3 on the domain $0 \leq \bar{x} \leq 1$ for the case when $u(0) = 1$ and $u(1) = 0$, which is given by

$$u(x) = \frac{1 - e^{Pe(1-x)}}{1 - e^{Pe}} \quad . \tag{4.9}$$

and for which two values of Pe, the Peclet number, are used: $Pe = 50$, the advection-dominated case which produces a sharp boundary layer (see Figure 4.1) and $Pe = 5$, the diffusion-dominated case which produces a smooth solution (see Figure 4.2). The third function used is $\sin x$ on the interval $-2\pi \leq x \leq 2\pi$ (see Figure 4.3).

When using a coarse grid the advection-dominated solution proved the most trouble, producing a solution which was unable to capture the sharp boundary layer (see, for example, Figure 4.4 which shows $< f'' >$ under these conditions). This problem was mitigated when the grid resolution was increased (see Figure 4.5). The coarse grid performed well for the diffusion-dominated case (see Figure 4.6) and for $\sin x$ (see Figure 4.7).

In tests of the behavior of the error with respect to the shape function support radius, r, the SPH approximations produced convergent results for all test functions. For example, Figure 4.8 shows the convergence when approximating the second gradient on each of the test functions. The error converges quadratically until r reaches a small enough number at which point the error starts to diverge. This is because shape function calculations approach machine precision (32-bit on our test machine).

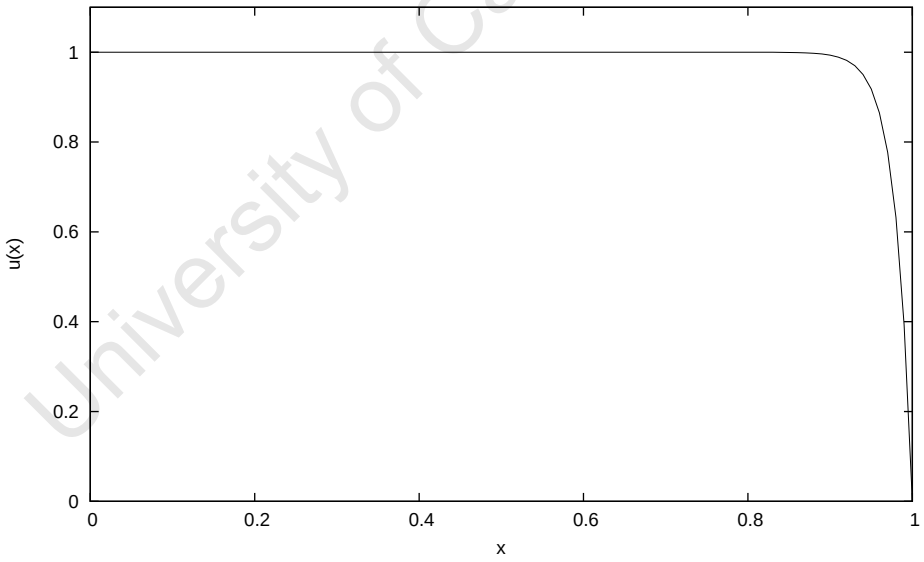

FIGURE 4.1: Exact solution to the advection-diffusion equation for $Pe = 50$

4.3.2 Behaviour with respect to choice of shape function

There wasn't much difference in function approximations when using a standard shape function (e.g. the quintic spline) and its derivatives as opposed to using the new shape functions (i.e. the piecewise-linear shape functions defined in Chapter 2). For example,

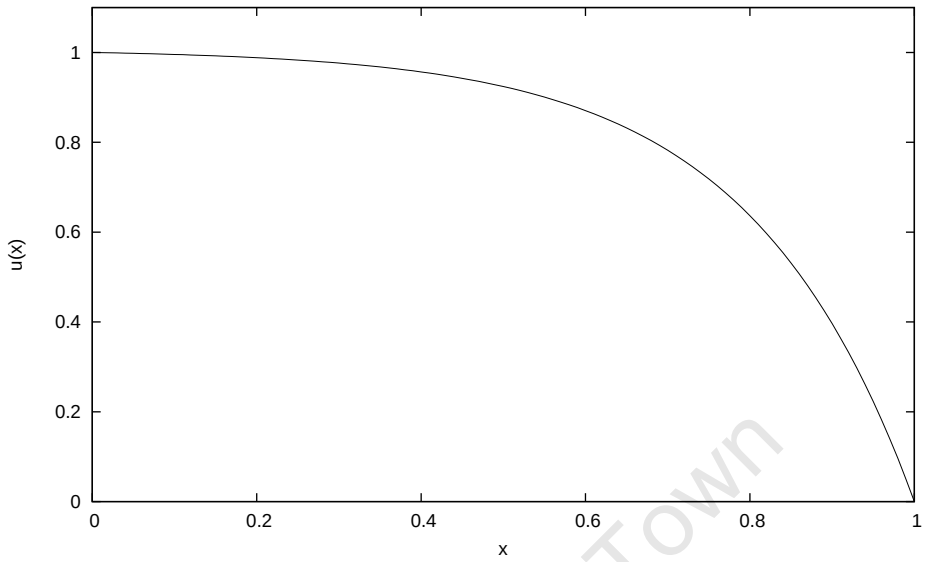

FIGURE 4.2: Exact solution to the advection-diffusion equation for $Pe = 5$

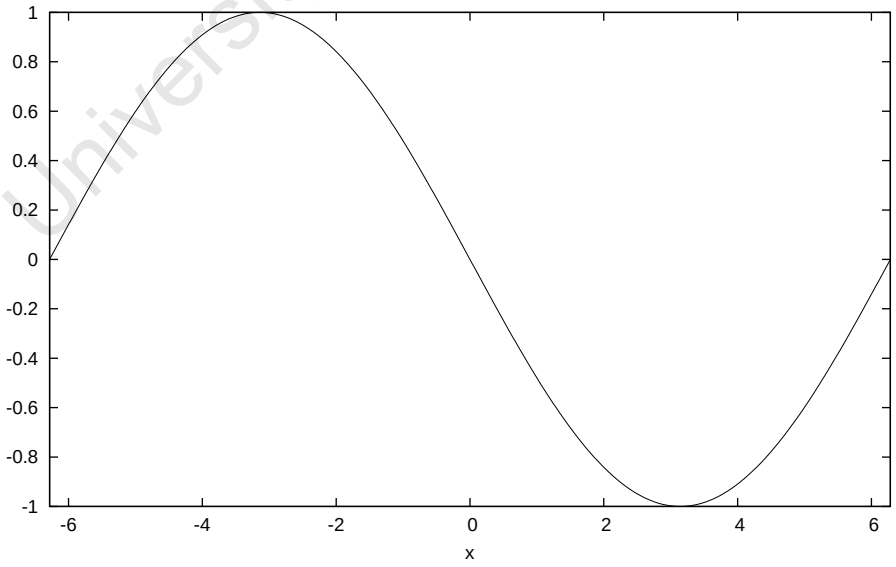

FIGURE 4.3: $\sin x$ between the limits $-2\pi \leq x \leq 2\pi$

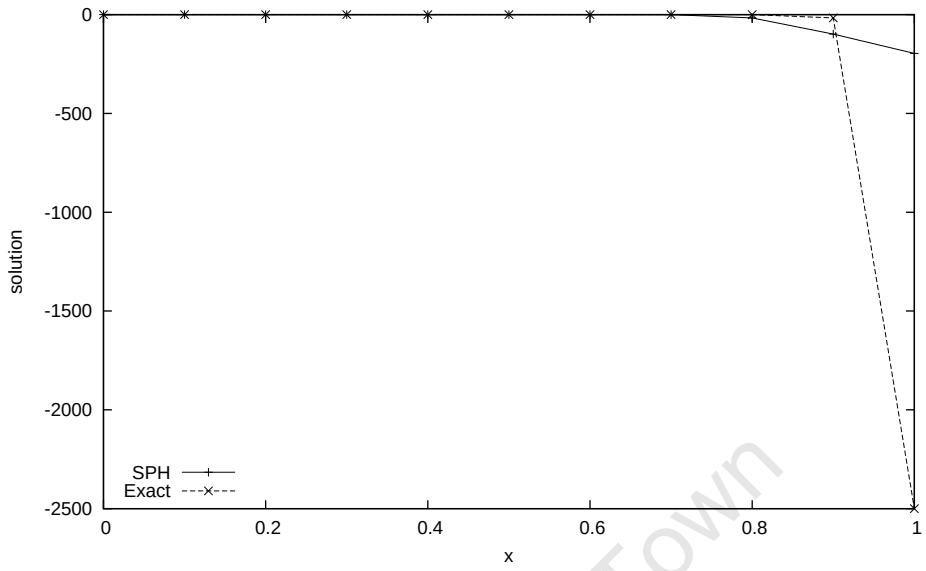

FIGURE 4.4: $< f'' >$ of the advection-diffusion equation solution for $Pe = 50$ when $N = 11$

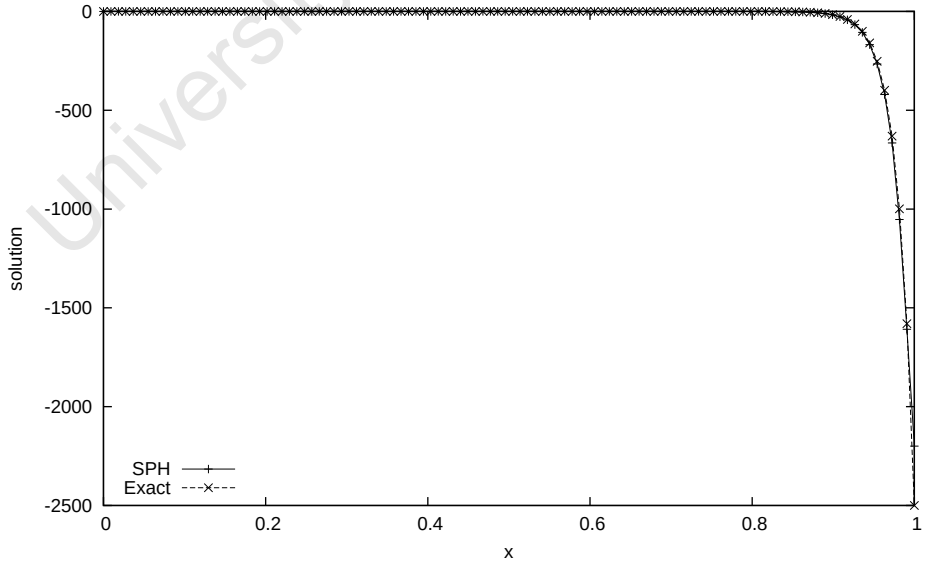

FIGURE 4.5: $< f'' >$ of the advection-diffusion equation solution for $Pe = 50$ when $N = 110$

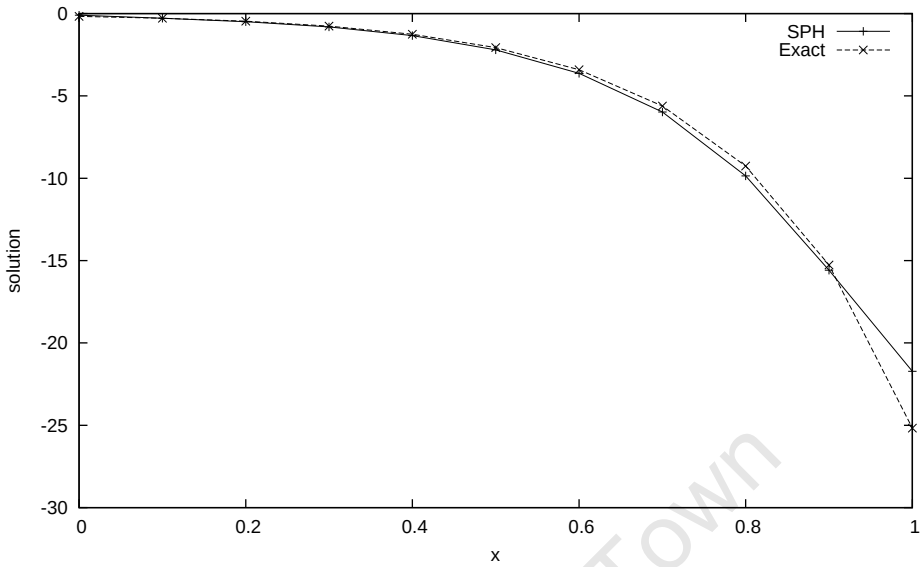

FIGURE 4.6: $< f'' >$ of the advection-diffusion equation solution for $Pe = 5$ when $N = 11$

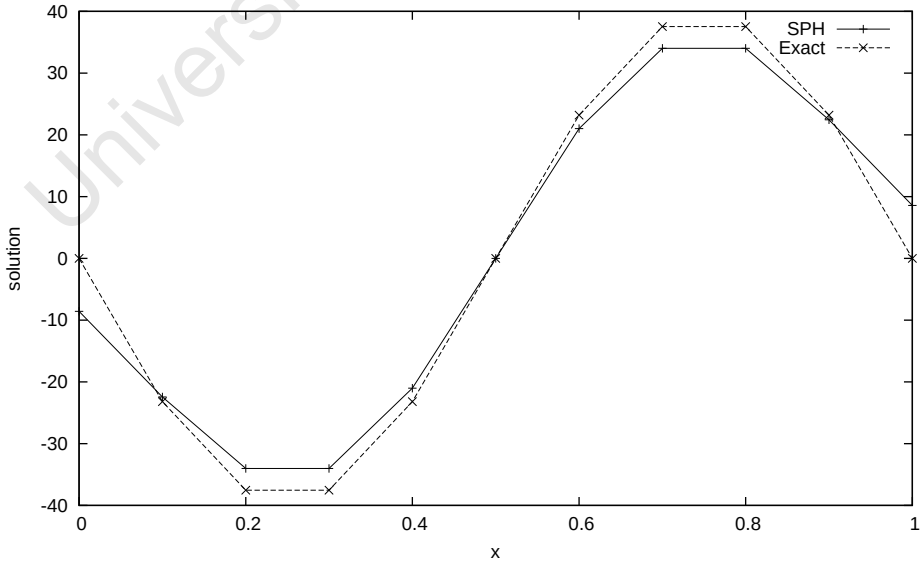

FIGURE 4.7: $< f'' >$ of $\sin x$ for $N = 11$

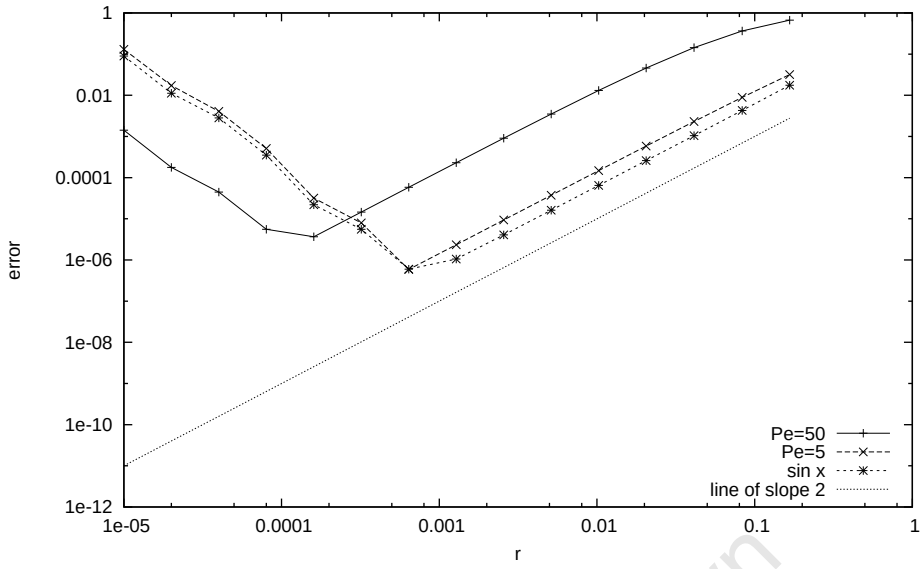

FIGURE 4.8: Convergence of $< f'' >$ for various f

Figure 4.9 shows the convergence with respect to r of the SPH approximations to the second derivative of the advection-diffusion equation solution for when $Pe = 50$, i.e. the advection-dominated case, using both shape functions. As can be seen, both achieved quadratic convergence with solutions breaking down when calculations reached machine precision, as before. Similar results were found when approximating the diffusion-dominated case (see Figure 4.10) and also when approximating $\sin x$ (see Figure 4.11).

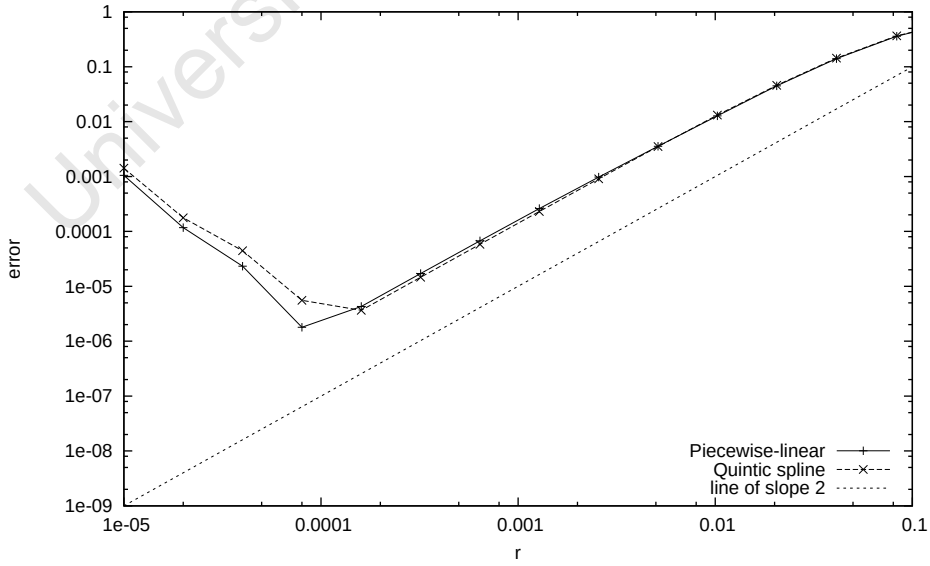

FIGURE 4.9: Convergence of $< f'' >$ of the advection-diffusion equation solution for $Pe = 50$ using different shape functions

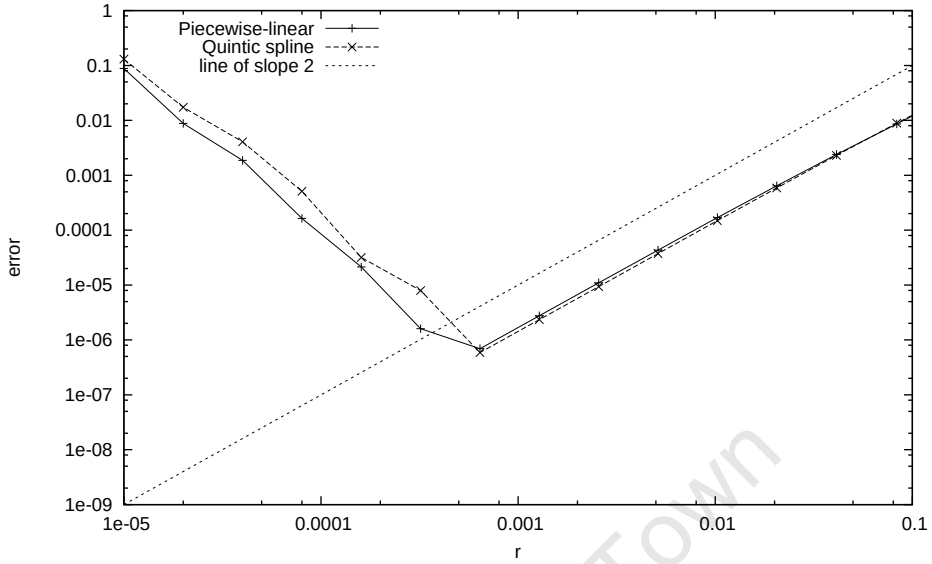

FIGURE 4.10: Convergence of $< f'' >$ of the exact solution to the advection-diffusion equation for $Pe = 5$ using different shape functions

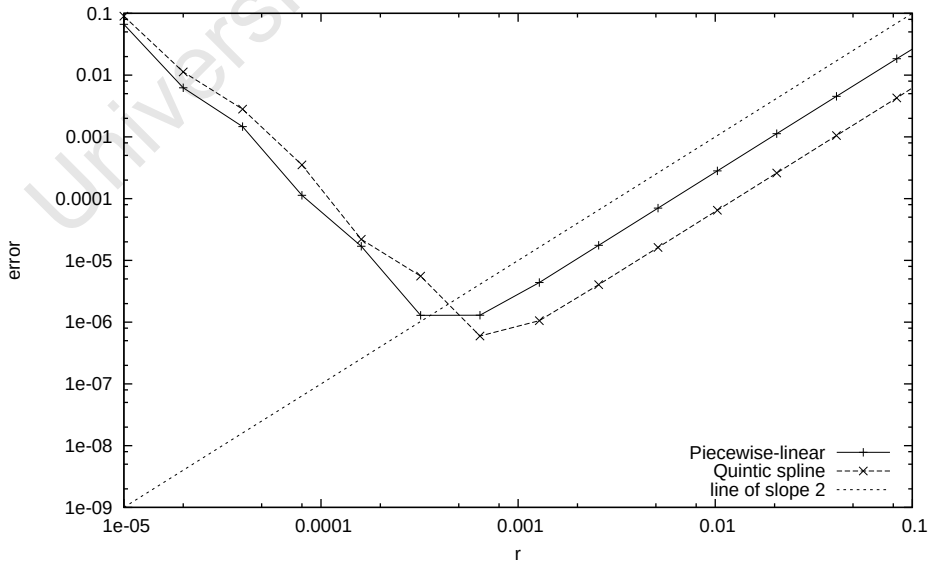

FIGURE 4.11: Convergence of $< f'' >$ of $\sin x$ using different shape functions

4.3.3 Behaviour with respect to quadrature

In convergence tests the rectangular rule and the trapezoidal rule reached a threshold error whilst Simpson's rule did not. For example, Figure 4.12 shows the convergence of $< f'' >$ with respect to r of the advection-diffusion equation solution, $Pe = 50$, using each quadrature technique. In addition, as n_r was increased so the limiting error decreased. See, for example, Figure 4.13 which shows this for the rectangle rule. This is in line with the theory outlined in Section 2.7 where it is shown that the discretisation error is dependent on $\Delta x/r$ (which is equivalent to $1/(2n_r + 1)$). Similar results where found when using the trapezoidal rule (see Figure 4.14). Simpson's rule produced no such result, however, and converged without a limit regardless of n_r (see Figure 4.15).

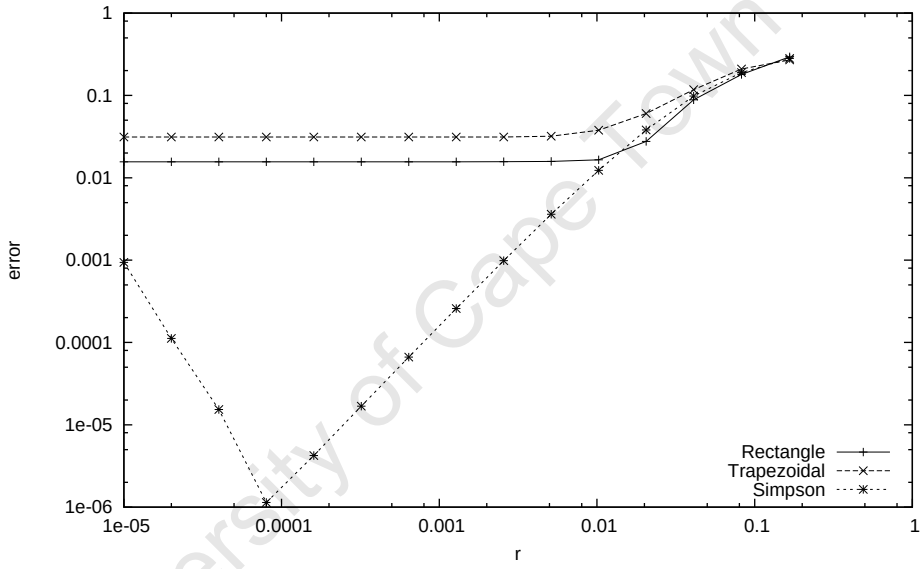

FIGURE 4.12: Convergence of $< f'' >$ of the advection-diffusion equation solution when $Pe = 50$ using various quadrature techniques

By setting $\Delta x/r = cr$, c is some constant, we can ensure that as $r \to 0$ so $\Delta x/r \to 0$. In this way we can ensure that the discretisation error vanishes with r. Figure 4.16 shows the convergence of $< f'' >$ on the advection-diffusion equation solution for $Pe = 50$ when $\Delta x/r = 2r$. As can be seen, quadratic convergence is achieved with no limiting error. However, as r decreases so the total number of particles increases quadratically which makes this technique very numerically expensive.

Finally, a further result of note is that the error diverges with respect to r unless n_r divided the shape function up along where the piecewise-defined functions met. That is, $n_r \propto c+1$ where c is the number of parts to the function on one side. For example, a quintic spline consists of three sections on either side, each covering a third of the function space. In our tests we found that when using a quintic spline we had to ensure that

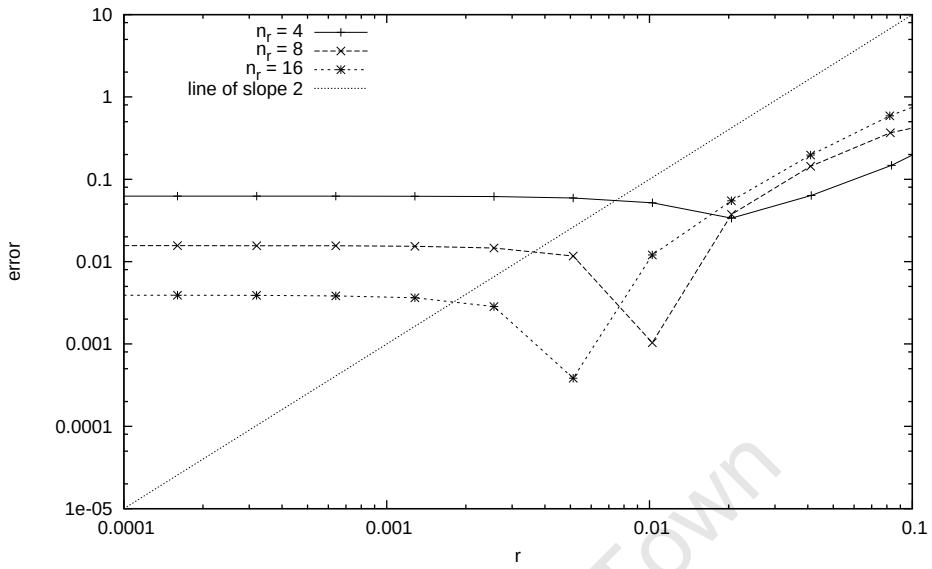

FIGURE 4.13: Convergence of $< f'' >$ of the advection-diffusion equation solution when $Pe = 50$ using rectangle-rule integration for different values of n_r

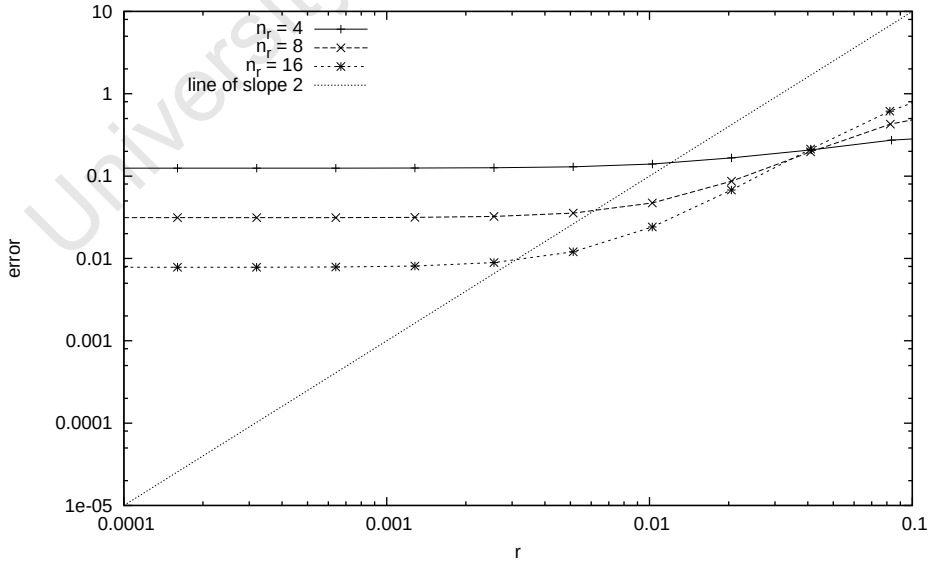

FIGURE 4.14: Convergence of $< f'' >$ of the advection-diffusion equation solution when $Pe = 50$ using trapezoidal integration for different values of n_r

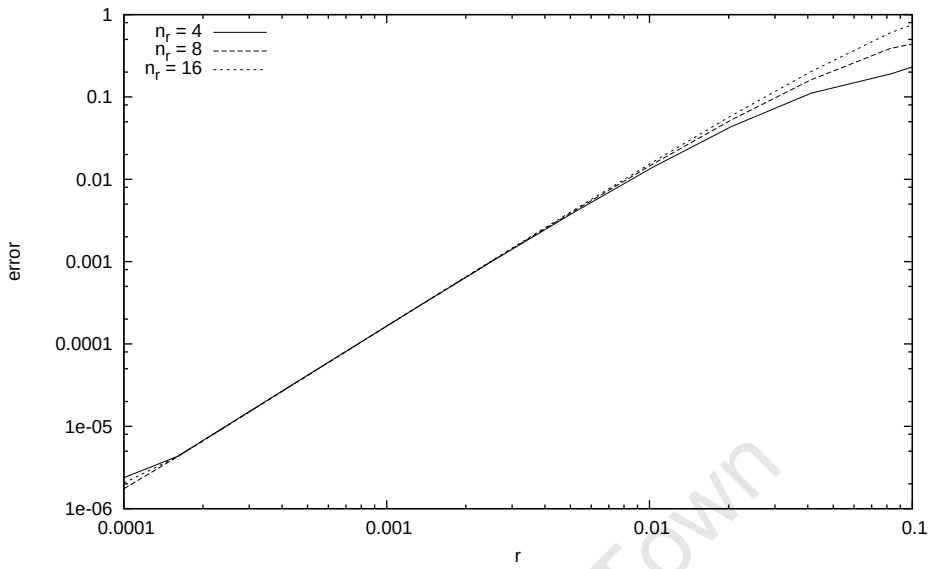

FIGURE 4.15: Convergence of $< f'' >$ of the advection-diffusion equation solution when $Pe = 50$ using simpson's integration for different values of n_r

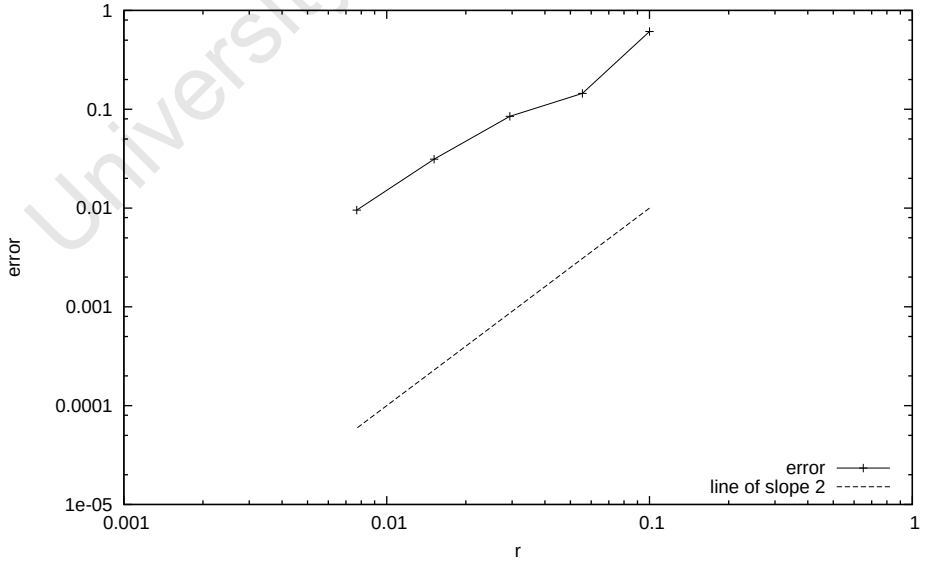

FIGURE 4.16: Convergence of $< f'' >$ of the advection-diffusion equation solution for $Pe = 50$ when $\Delta x/r = 2r$

$n_r \propto 4$. For example, Figure 4.17 shows the convergence of $< f'' >$ for different values of n_r using a quintic spline. As can be seen, the error diverged when the proportionality condition was not met. Similarly for the piecewise-linear shape functions. In that case we had to ensure that $n_r \propto 2$ when calculating $< f'' >$ since g_2 is a mod function defined once on either side (see Section 2.3). To illustrate, Figure 4.18 shows the same tests for differing values of n_r but using g_2 for the shape function. As one can see, the error diverged for odd values of n_r. There is, as of yet, no explanation for this behaviour.

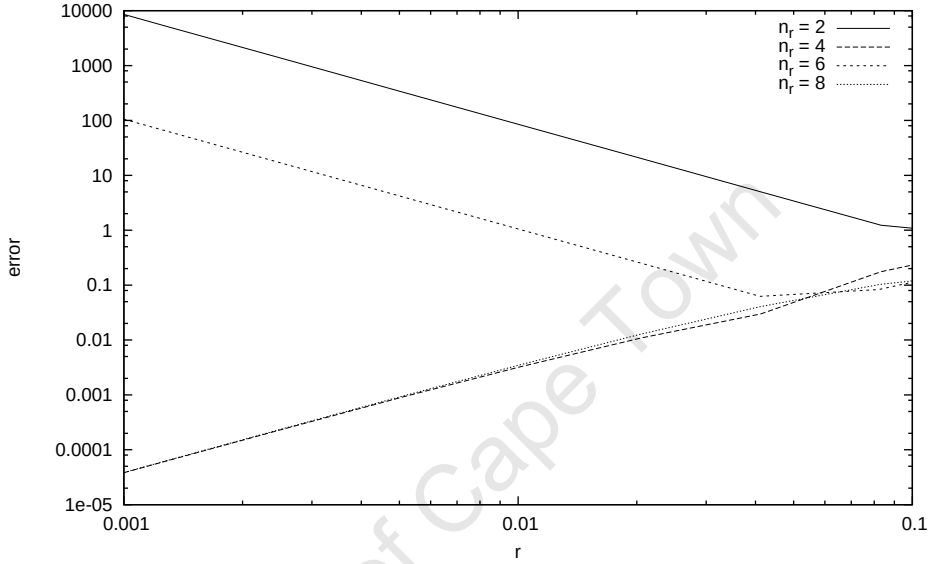

FIGURE 4.17: Convergence of $< f'' >$ of the advection-diffusion equation solution when $Pe = 50$ using a quintic spline shape function with different values of n_r

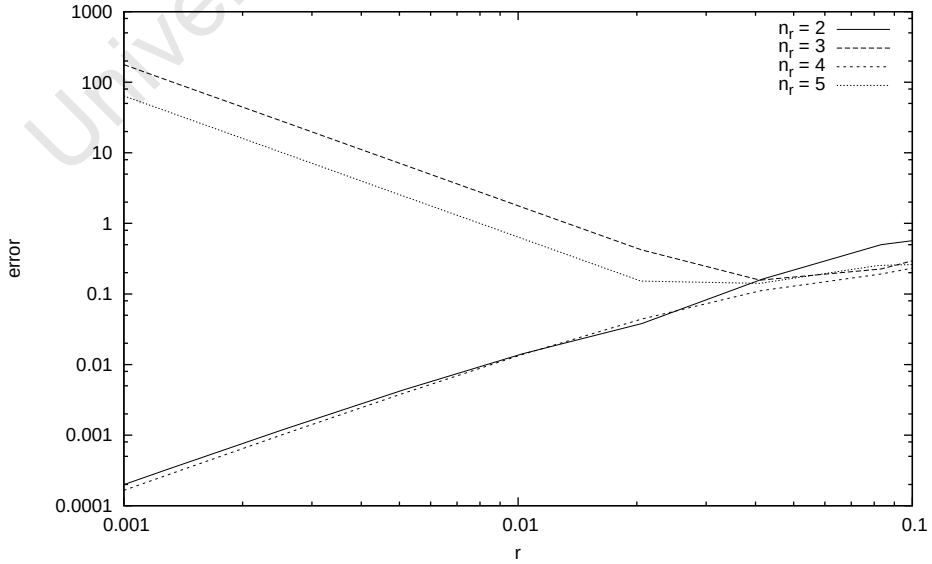

FIGURE 4.18: Convergence of $< f'' >$ of the advection-diffusion equation solution when $Pe = 50$ using the piecewise-linear shape function with different values of n_r

4.3.4 Domain extension

We used Lagrange polynomials to extend the domain so that we could ensure continuity at the boundary of any desired order. In Section 2.5 we suggested that nth-order continuity was required when approximating $f^{(n)}$. This is exactly what we found. For example, Figure 4.19 shows the approximation of $< f' >$ using varying levels of continuity at the boundary. With first-order continuity at the boundary we get first-order convergence. When we use zero-order continuity the method fails to converge. Similarly for the second gradient: when using first-order continuity at the boundary the method does not converge whilst with second-order continuity it does (see Figure 4.20).

Another point to note is that quadratic convergence was only achieved when continuity was of order $n + 1$. That is, when approximating $< f' >$ first-order continuity produced an error of order 1 whilst second-order continuity produced an error of order 2. Similarly, when approximating $< f'' >$ which produced an error of order 1 with second-order continuity and an error of 2 with third-order continuity. However, as can be seen, in both cases increasing the continuity further did not increase the order of convergence.

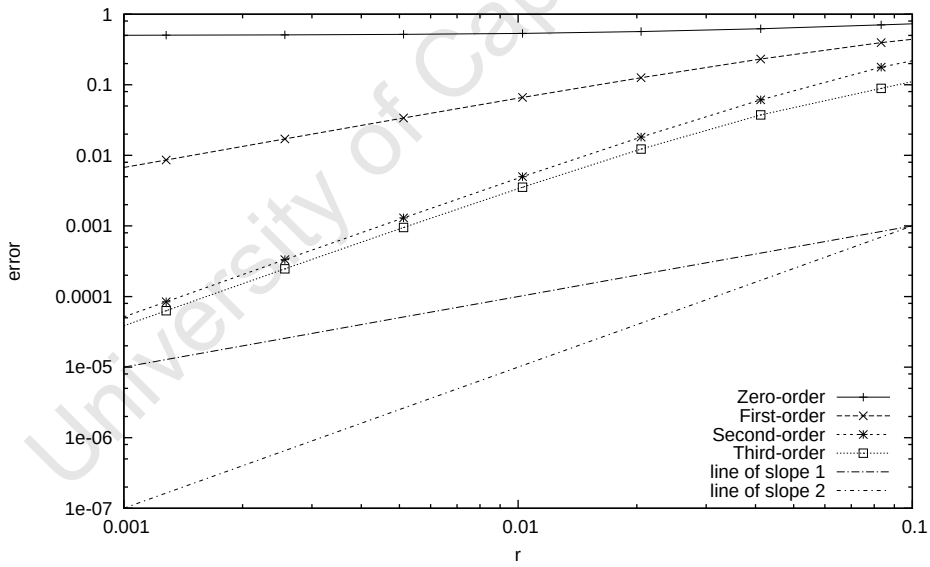

FIGURE 4.19: Convergence of $< f' >$ of the advection-diffusion equation solution when $Pe = 50$ for varying levels of continuity at the boundary

4.4 Solving the advection-diffusion equation

To solve the advection-diffusion equation we start by writing out the strong form of the equation

$$u'(x) - ku''(x) = 0 \ , \quad a \leq x \leq b \ , \quad u(a) = 1, \ u(b) = 0 \ , \tag{4.10}$$

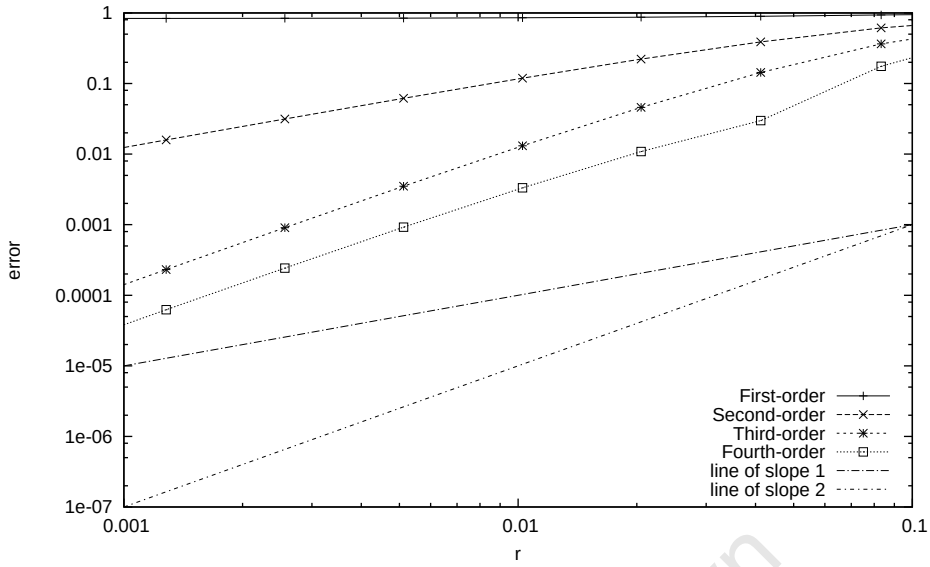

FIGURE 4.20: Convergence of $< f'' >$ of the advection-diffusion equation solution when $Pe = 50$ for varying levels of continuity at the boundary

where $u' \equiv du/dx$ and $u'' \equiv d^2u/dx^2$. Next we apply the smoothed approximation to each term to get

$$<\tilde{u}'>(x) - \ k <\tilde{u}''>(x) \ = \ 0 \ , \quad a \leq x \leq b \ , \tag{4.11}$$

where $\tilde{u}$ is the form of u extended at the boundaries. This is equivalent to writing

$$\int_{x-r}^{x+r} \tilde{u}(\xi) g_1(\xi - x) d\xi \ - \ k \int_{x-r}^{x+r} \tilde{u}(\xi) g_2(\xi - x) d\xi \ = \ 0 \ , \quad a \leq x \leq b \quad , \tag{4.12}$$

thus using g_1 for the first term and g_2 for the second. We now replace (4.12) with its discrete approximation. Using the rectangle rule this becomes

$$\sum_{i=j-n_r}^{j+n_r} \Big[\tilde{u}(x_i) g_1(x_i - x_j) - k\tilde{u}(x_i) g_2(x_i - x_j) \Big] \Delta x \ = \ 0 \ , \quad j = 0, 1, ...N-1 \tag{4.13}$$

where $x_i = a + i\Delta x$, $x_j = a + j\Delta x$, $\Delta x = (b-a)/(N-1)$ is the particle spacing, N is the number of particles in the domain and n_r is the number of particles on either side used to integrate the shape functions. To illustrate how we write this in vector form we

use the example of $N = 6$ and $n_r = 2$. Now (4.13) can be written as

$$\begin{bmatrix} S_{-2} & S_{-1} & S_0 & S_1 & S_2 & \cdot & \cdot & \cdot & \cdot & \cdot \\ \cdot & S_{-2} & S_{-1} & S_0 & S_1 & S_2 & \cdot & \cdot & \cdot & \cdot \\ \cdot & \cdot & S_{-2} & S_{-1} & S_0 & S_1 & S_2 & \cdot & \cdot & \cdot \\ \cdot & \cdot & \cdot & S_{-2} & S_{-1} & S_0 & S_1 & S_2 & \cdot & \cdot \\ \cdot & \cdot & \cdot & \cdot & S_{-2} & S_{-1} & S_0 & S_1 & S_2 & \cdot \\ \cdot & \cdot & \cdot & \cdot & \cdot & S_{-2} & S_{-1} & S_0 & S_1 & S_2 \end{bmatrix} \begin{bmatrix} \tilde{u}_{-2} \\ \tilde{u}_{-1} \\ \tilde{u}_0 \\ \tilde{u}_1 \\ \tilde{u}_2 \\ \tilde{u}_3 \\ \tilde{u}_4 \\ \tilde{u}_5 \\ \tilde{u}_6 \\ \tilde{u}_7 \end{bmatrix} = \begin{bmatrix} 0 \\ 0 \\ 0 \\ 0 \\ 0 \\ 0 \\ 0 \\ 0 \\ 0 \\ 0 \end{bmatrix} \tag{4.14}$$

where $S_i \equiv \Big[g_1(i\Delta x) - kg_2(i\Delta x)\Big]\Delta x$ and $\tilde{u}_j \equiv \tilde{u}(a + j\Delta x)$.

Now we need to impose the boundary conditions $\tilde{u}(a) = u_a$ and $\tilde{u}(b) = u_b$. We do this directly, so that (4.14) becomes

$$\begin{bmatrix} \cdot & \cdot & 1 & \cdot & \cdot & \cdot & \cdot & \cdot & \cdot & \cdot \\ \cdot & S_{-2} & S_{-1} & S_0 & S_1 & S_2 & \cdot & \cdot & \cdot & \cdot \\ \cdot & \cdot & S_{-2} & S_{-1} & S_0 & S_1 & S_2 & \cdot & \cdot & \cdot \\ \cdot & \cdot & \cdot & S_{-2} & S_{-1} & S_0 & S_1 & S_2 & \cdot & \cdot \\ \cdot & \cdot & \cdot & \cdot & S_{-2} & S_{-1} & S_0 & S_1 & S_2 & \cdot \\ \cdot & \cdot & \cdot & \cdot & \cdot & \cdot & \cdot & 1 & \cdot & \cdot \end{bmatrix} \begin{bmatrix} \tilde{u}_{-2} \\ \tilde{u}_{-1} \\ \tilde{u}_0 \\ \tilde{u}_1 \\ \tilde{u}_2 \\ \tilde{u}_3 \\ \tilde{u}_4 \\ \tilde{u}_5 \\ \tilde{u}_6 \\ \tilde{u}_7 \end{bmatrix} = \begin{bmatrix} 0 \\ 0 \\ u_a \\ 0 \\ 0 \\ 0 \\ 0 \\ u_b \\ 0 \\ 0 \end{bmatrix} \tag{4.15}$$

Finally we need to ensure that the values of $\tilde{u}$ outside of a and b are equal to the values of the Lagrange polynomial which extends u near the boundary to the sufficient degree (see Section 4.3.4 for more). We do this first by noting that $\tilde{u}_{0..5} \equiv u_{0..5}$ and then adding

4 lines to (4.15), one for each of the points outside of a and b,

$$\begin{bmatrix} 1 & \cdot & -l^a_{0,-2} & -l^a_{1,-2} & -l^a_{2,-2} & \cdot & \cdot & \cdot & \cdot & \cdot \\ \cdot & 1 & -l^a_{0,-1} & -l^a_{1,-1} & -l^a_{2,-1} & \cdot & \cdot & \cdot & \cdot & \cdot \\ \cdot & \cdot & 1 & \cdot & \cdot & \cdot & \cdot & \cdot & \cdot & \cdot \\ \cdot & S_{-2} & S_{-1} & S_0 & S_1 & S_2 & \cdot & \cdot & \cdot & \cdot \\ \cdot & \cdot & S_{-2} & S_{-1} & S_0 & S_1 & S_2 & \cdot & \cdot & \cdot \\ \cdot & \cdot & \cdot & S_{-2} & S_{-1} & S_0 & S_1 & S_2 & \cdot & \cdot \\ \cdot & \cdot & \cdot & \cdot & S_{-2} & S_{-1} & S_0 & S_1 & S_2 & \cdot \\ \cdot & \cdot & \cdot & \cdot & \cdot & \cdot & \cdot & 1 & \cdot & \cdot \\ \cdot & \cdot & \cdot & \cdot & \cdot & \cdot - l^b_{2,1} & -l^b_{1,1} & -l^b_{0,1} & 1 & \cdot \\ \cdot & \cdot & \cdot & \cdot & \cdot & \cdot - l^b_{2,2} & -l^b_{1,2} & -l^b_{0,2} & \cdot & 1 \end{bmatrix} \begin{bmatrix} \tilde{u}_{-2} \\ \tilde{u}_{-1} \\ u_0 \\ u_1 \\ u_2 \\ u_3 \\ u_4 \\ u_5 \\ \tilde{u}_6 \\ \tilde{u}_7 \end{bmatrix} = \begin{bmatrix} 0 \\ 0 \\ u_a \\ 0 \\ 0 \\ 0 \\ 0 \\ u_b \\ 0 \\ 0 \end{bmatrix} \tag{4.16}$$

where the first two rows ensure that $\tilde{u}_{-2}$ and $\tilde{u}_{-1}$ are the values of the Lagrange polynomial which interpolates u_0, u_1 and u_2, and the last two rows ensure that $\tilde{u}_6$ and $\tilde{u}_7$ do so similarly for u_3, u_4 and u_5, both using $l^a_{i,j}$ for the first and $l^b_{i,j}$ for the second where i describes which of the Lagrange co-efficients are being used and j which particle, $l^a_{i,j} \equiv l_i(a - j\Delta x)$ and $l^b_{i,j} \equiv l_i(b - j\Delta x)$.

Thus we have a linear system of equations which can be written as

$$Su = F \tag{4.17}$$

which can be solved for u.

4.4.1 Test problems

Tests are performed on the advection-diffusion problem on the domain $0 \leq x \leq 1$ for the case when $u(0) = 1$ and $u(1) = 0$, which has solution

$$u(x) = \frac{1 - e^{Pe(1-x)}}{1 - e^{Pe}} \quad , \tag{4.18}$$

for the case when $Pe = 50$, which produces a sharp boundary layer (see Figure 4.1), and for when $Pe = 5$ which produces a smooth, diffusion-dominated solution (see Figure 4.2).

Using a coarse grid of eleven particles the solution was poor for the advection-dominated case (see Figure 4.21). This was mitigated by increasing the grid resolution (see Figure 4.22). In the diffusion dominated case the solution was good even with a coarse grid (see Figure 4.23). In both cases, however, quadratic convergence was achieved with respect

to r until r became less than 0.001 at which point the convergence broke down (see Figure 4.24).

To illustrate this issue, Figure 4.25 shows the plot of the solution of the aformentioned tests when $r = 0.005$ whilst Figure 4.26 shows the solution when $r = 0.001$. As can be seen, when $r = 0.005$ the technique produced a good approximation to the exact solution but when $r = 0.001$ the solution completely breaks down. Using Hager's conditioning algorithm [34] we calculate the conditioning number in the first case to be 4.23×10^{13} and in the second 6.57×10^{16}. Since the value of machine precision on our test machine was of order 4.5×10^{15} it seems clear that the breakdown is caused by an ill conditioning in the linear system. It is not, however, understood why the conditioning is so poor and is left as a question for future work.

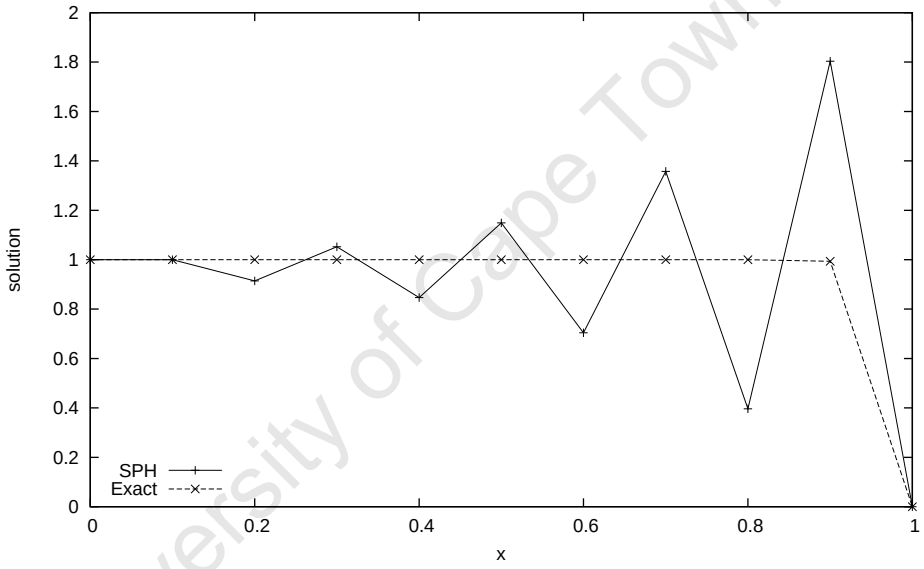

FIGURE 4.21: SPH solution to the advection-diffusion equation for $Pe = 50$ when $N = 11$

4.4.2 Behaviour with respect to choice of shape functions

Both the standard SPH technique, that is, using a single shape function and its derivatives, and the new, piecewise-linear shape functions, that is, using different shape functions for each derivative, produced similar convergence with respect to r when solving the boundary value problems. Figure 4.27 shows the convergence when $Pe = 50$ using both the quintic spline and its derivatives and when using the various piecewise-linear shape functions. As can be seen, both techniques converged with r^2 but the results broke down as r reached a small enough number, as before (see previous section for more on this).

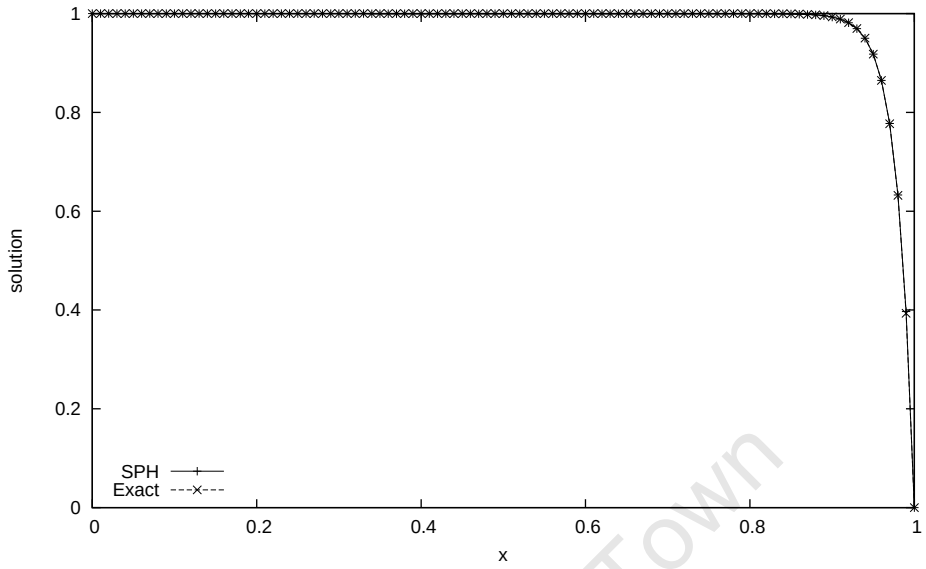

FIGURE 4.22: SPH solution to the advection-diffusion equation for $Pe = 50$ when $N = 110$

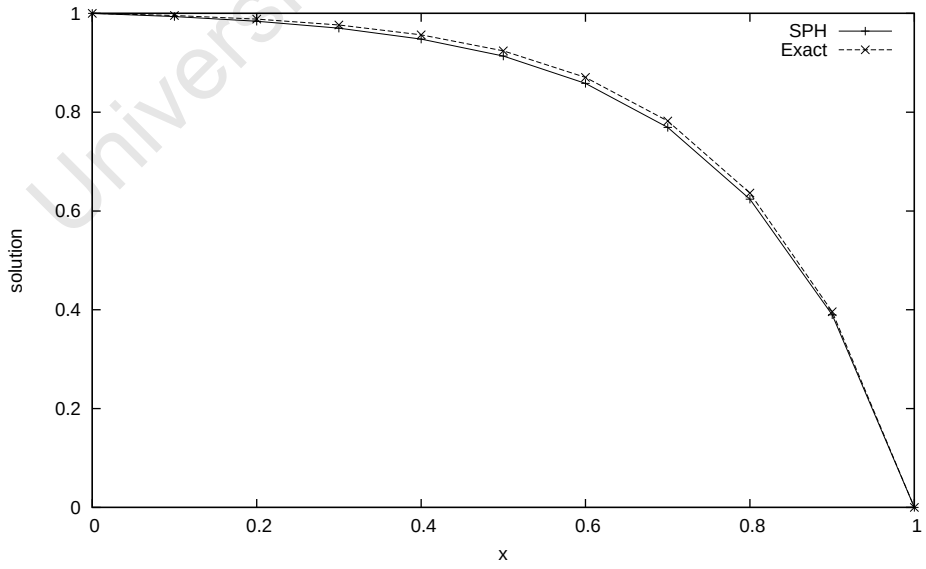

FIGURE 4.23: SPH solution to the advection-diffusion equation for $Pe = 5$ and $N = 11$

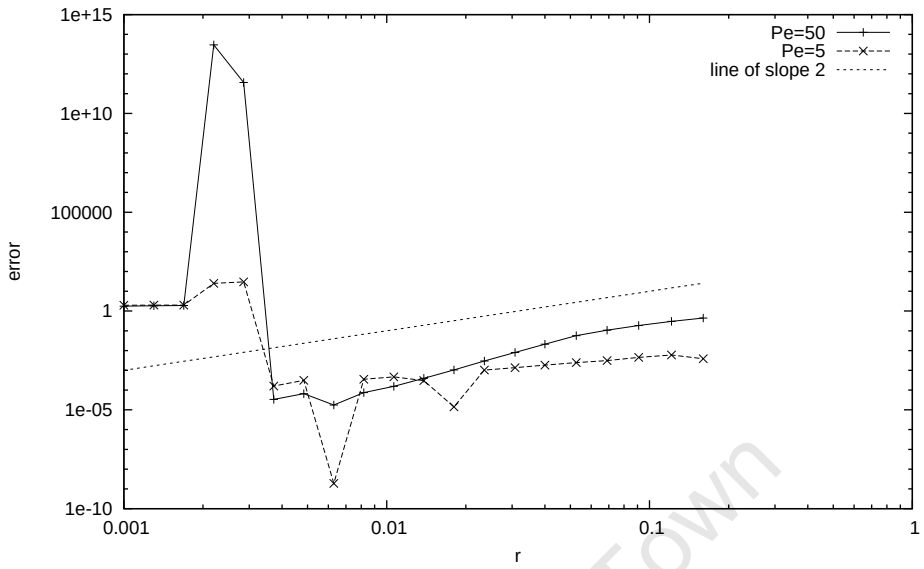

FIGURE 4.24: Convergence of SPH solutions to the advection-diffusion equation for $Pe = 50$ and $Pe = 5$

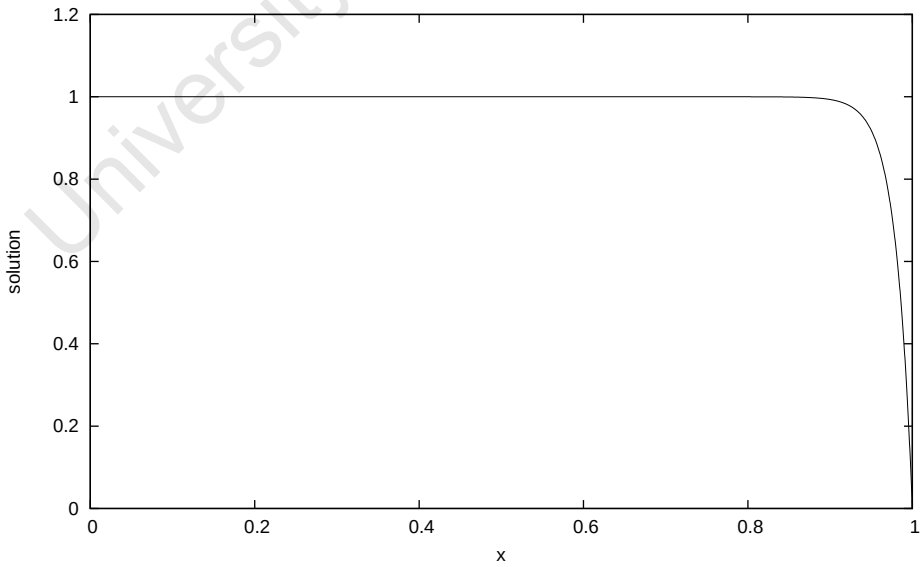

FIGURE 4.25: SPH solution to the advection-diffusion equation for $Pe = 50$ when $r = 0.005$

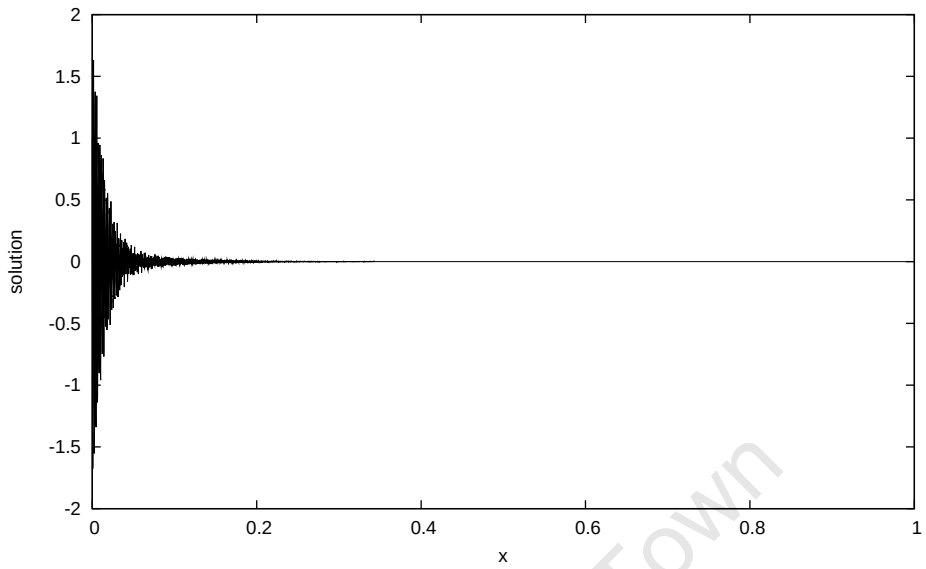

FIGURE 4.26: SPH solution to the advection-diffusion equation for $Pe = 50$ when $r = 0.001$

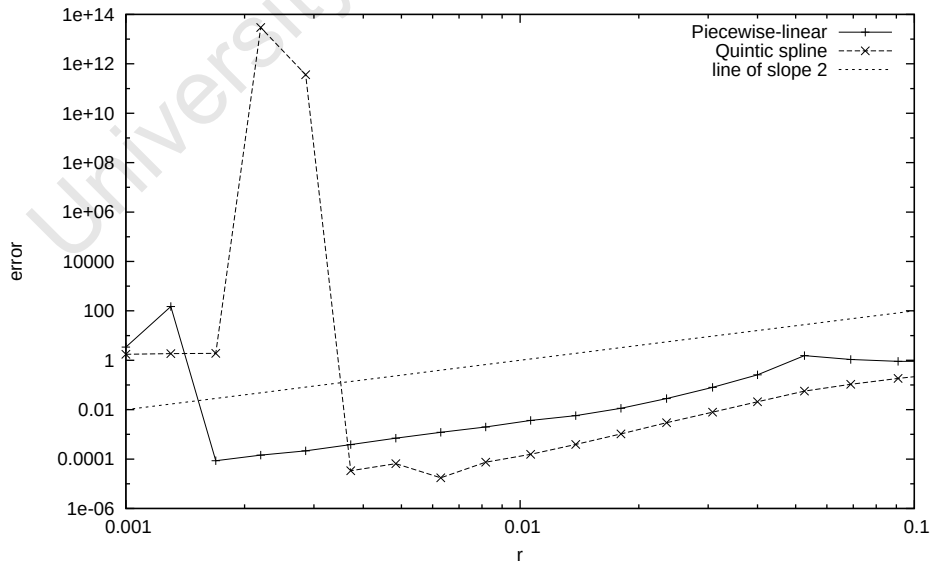

FIGURE 4.27: Convergence of SPH solutions to the advection-diffusion equation for $Pe = 50$ using different shape function techniques

4.4.3 Behaviour with respect to quadrature rule

We use three different quadrature techniques: the rectangle rule, the trapezoidal rule and Simpson's rule (see Section 4.2 for more on these). All the techniques converged quadratically when solving the boundary value problem. For example, Figure 4.28 shows the convergence of each when $Pe = 50$. However, convergence was sensitive to the number of particles under the cover, n_r. As explained in Section 4.3.3, when using the quintic spline convergence only occurred when $n_r \propto 4$ (see Figure 4.29) whilst when using the piecewise-linear functions it only occurred when $n_r \propto 2$ (see Figure 4.30).

Finally, as in Section 4.3, we tested convergence behaviour when $\Delta x/r = 2r$. In this case better than quadratic convergence was achieved (see Figure 4.31).

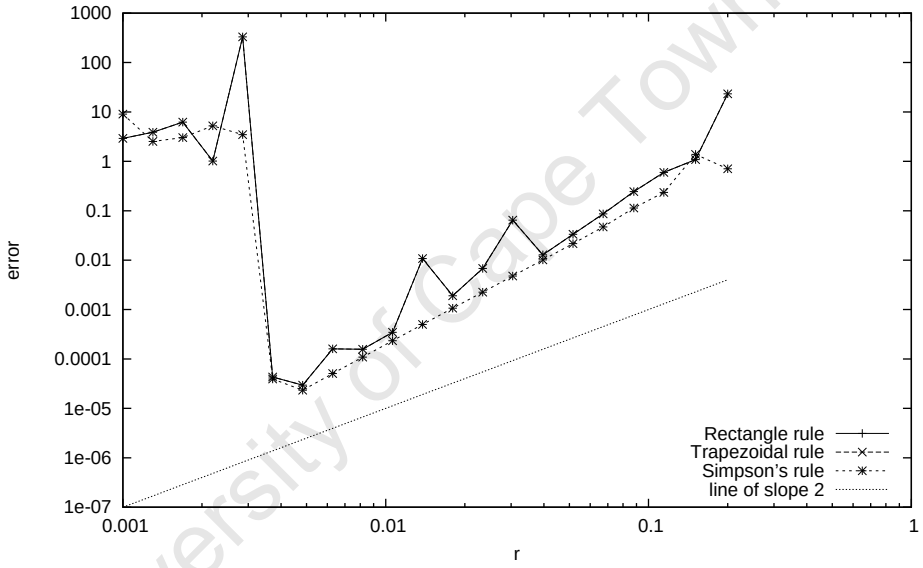

FIGURE 4.28: Convergence of SPH solutions to the advection-diffusion equation for $Pe = 50$ using various quadrature techniques

4.4.4 Domain extension

In Chapter 3 we predicted that we needed at least second-order continuity to solve the boundary value problems. However, we found that only first-order continuity was required to produce convergent results (see Section 4.1 for more on the extension technique and Section 4.4 on how this was applied to solving a boundary value problem). For example, Figure 4.32 shows the convergence of error with varying levels of continuity enforced at the boundary. As can be seen, increasing the continuity increases the rate of convergence. And as before, the results break down at small values of r. This is, again, due to ill-conditioning of the system matrix (see Section 4.4.1 for more on this).

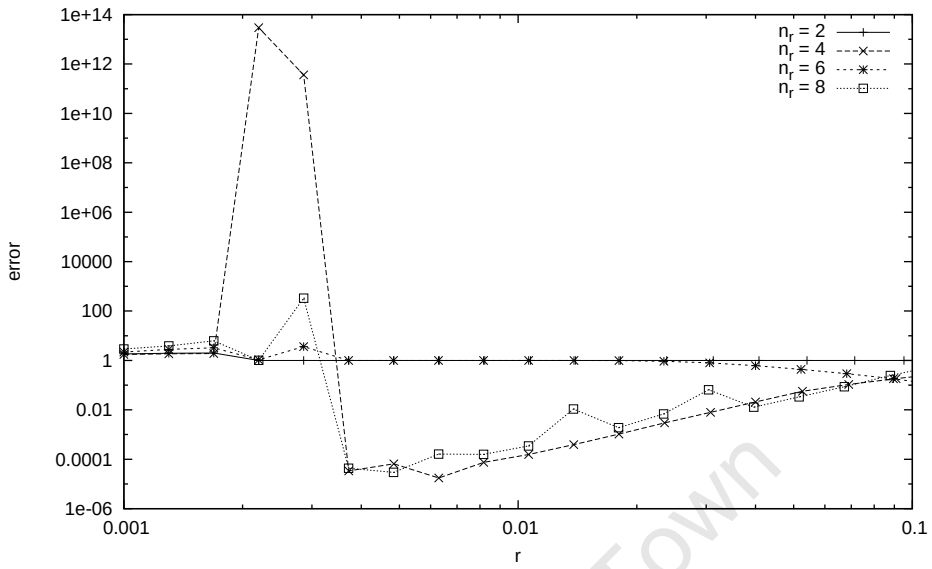

FIGURE 4.29: Convergence of SPH solutions to the advection-diffusion equation for $Pe = 50$ using the quintic spline with various values of n_r

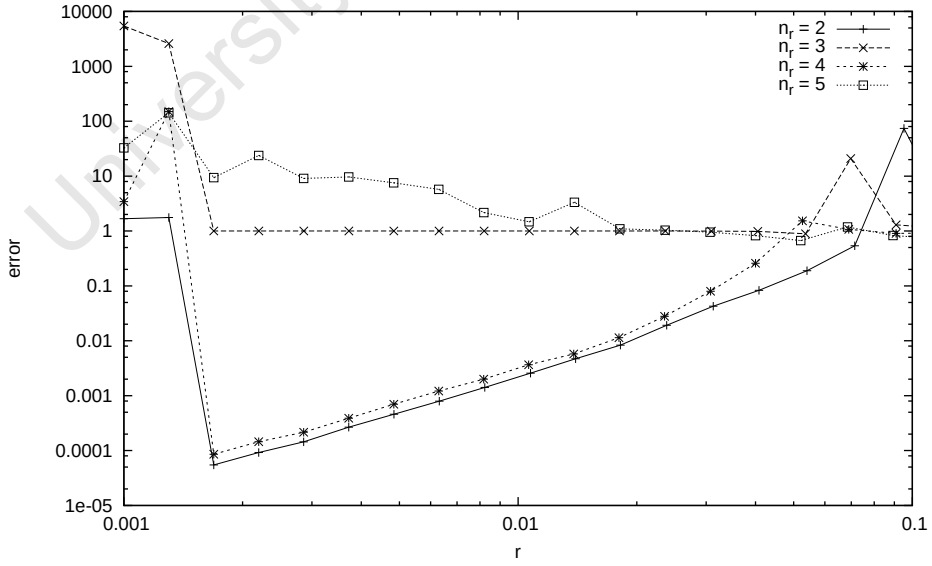

FIGURE 4.30: Convergence of SPH solutions to the advection-diffusion equation for $Pe = 50$ using the piecewise-linear shape functions with various values of n_r

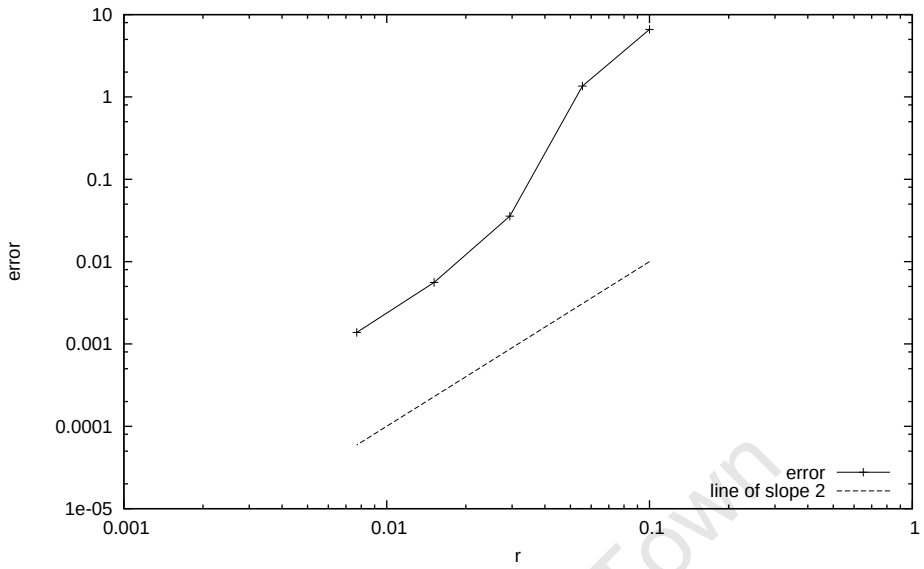

FIGURE 4.31: Convergence of SPH solutions to the advection-diffusion equation for $Pe = 50$ when $\Delta x/r = 2r$

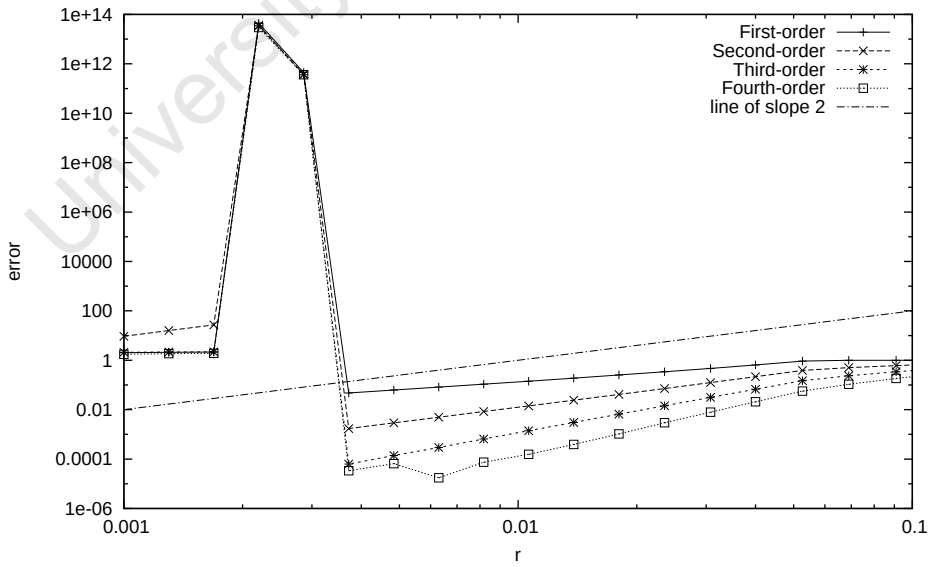

FIGURE 4.32: Convergence of SPH solutions to the advection-diffusion equation for $Pe = 50$, enforcing varying levels of continuity at the boundary

Chapter 5

Conclusions and future work

In this thesis we carried out a study of the properties of SPH approximation in one space dimension, paying particular attention to consistency and convergence. We have developed a new approach to formulating consistent approximations to derivatives which is more general than the formulation normally used. From this it has been shown how piecewise-linear shape functions can be used both to approximate functions and their derivatives and also to solve boundary value problems (in this case, the advection-diffusion equation).

Various analyses and results presented here corroborate the findings of Quinlan et al. [20]. By deriving an estimate for the total error in SPH approximations we show that convergent and consistent results are only possible by both reducing the size of the shape function cover, i.e. r, and simultaneously reducing the relative particle spacing $\Delta x/r$. However, when using Simpson's rule for quadrature this was not the case in that the use of this rule produced results which converged with respect to r, independently of $\Delta x/r$. This has yet to be explained but holds the promise of interesting future work. A drawback of Simpson's rule, though, is that it would not work for non-uniform particle spacing.

Quadrature is probably the biggest open question left by this thesis. Though an analysis of the error for the rectangle rule was performed, this has yet to be done for the trapezoidal rule and Simpson's rule. Also, it is not understood why the quadrature points had to coincide with the boundaries of the piecewise-defined shape functions (see Section 4.3.3). This is the largest limiting factor for the usefulness of the methods described here since it means that convergent results cannot be produced for arbitrary particle distributions. Producing a singularly defined function using the new approach may mitigate this issue.

Perhaps the most pertinent original result in this thesis was the discovery that in order to produce consistent and convergent approximations to the nth derivative one must ensure n-order continuity at the boundary. This was shown analytically and confirmed experimentally (using Lagrange polynomials). This fact has, to our knowledge, never been stated in literature.

Both the diffusion-dominated and the advection-dominated case of the advection-diffusion equation converged equally well, which is what one would expect. However, the issue of accuracy for relatively coarse particle distributions has not been dealt with in this work, which awaits extensions analogous to the SUPG method of [12]. Atluri [11] has in this regard developed a meshless analogy to SUPG which would be an interesting avenue to take in future work once the current issues with the method have been resolved.

Finally, other future work would have to include fixing the poor conditioning of the matrices used in solving the boundary value problems. At this point the methods described could only be used on a system of around ten thousand particles per axis, or less. Also, the application to higher space dimensions needs to be considered. The most important work to be done, however, is to investigate the conditions under which approximations will converge under arbitrary particle distributions. As mentioned, the methods described here are highly sensitive to relative particle positions, even for the uniform case, and are thus not ready for general use. However, were this issue resolved SPH could be developed into a powerful general technique for solving differential equations.

Bibliography

[1] L. Lucy. A numerical approach to the fission hypothesis. *Astronomical Journal*, 82: 1013

[2] R. A. Gingold and J.J. Monaghan. Smoothed particle hydrodynamics: theory and applications to N-n-spherical stars. *Notices of the Royal Astronomical Society*, 181:375

[3] T. Liszka and J. Orkisz. Modified finite difference methods at arbitrary irregular meshes and its application. *Applied Mechanics, Proceedings Of the 18th Polish Conference On Mechanics of Solids*, Wisla, Poland (1976)

[4] D. Fulk and D. Quinn. An analysis of 1-d smoothed particle hydrodynamics kernels. *Journal of Computational Physics*, volume 126 (1990), p. 165-180

[5] J. K. Chen, J. E. Beraun, and T. C. Carney. A corrective smoothed particle method for boundary value problems in heat conduction. *International Journal for Numerical Methods in Engineering*, 46, 231-252 (1999)

[6] Li Shaofan and Wing Kam Liu, Meshfree particle methods. 1st ed. 2004. Corr. 2nd printing, 2007, VIII, 502 p., Hardcover, ISBN: 978-3-540-22256-9

[7] E. W. Weisstein. Delta function. From MathWorld–A Wolfram Web Resource. http://mathworld.wolfram.com/DeltaFunction.html

[8] H. F. Schwaiger. An implicit corrected SPH formulation for thermal diffusion with linear free surface boundary conditions. *International Journal for Numererical Methods in Engineering*, 2008, 75:647671

[9] L. Brookshaw. A method of calculating radiative heat diffusion in particle simulations. *Proceedings of the Astronomical Society of Australia*, 1985; 6(2):207-210.

[10] T. Belytschko, Y. Krongaux, D. Organ, M. Fleming, and P. Krysl. Meshless methods: an overview and recent developments. *Computational Methods in Applied Mechanics and Engineering*, 139 (1996) 347

[11] H. Lin and S. N. Atluri. Meshless local Petrov-Galerkin (MLPG) method for convection-diffusion. *CMES-Computer Modeling in Engineering & Sciences*, 1 (2): 45-60, 2000

[12] A. N. Brooks and T. J. R. Hughes. Streamline upwind/Petrov-Galerkin formulations for convection dominated flows with particular emphasis on the incompressible Navier-Stokes equations. *Computational Methods in Applied Mechanics and Engineering*, 32 (1982), p. 199

[32] J. Hongbin and D. Xin. On criterions for smoothed particle hydrodynamics kernels in stable field *Journal of Computational Physics*, Volume 202, Issue 2, 20 January 2005, Pages 699-709

[14] J. W. Swegel, D. L. Hicks, and S. W. Attaway. Smoothed particle hydrodynamics stability analysis. *Journal of Computational Physics*, Volume 116, Issue 1, January 1995, Pages 123-134

[15] G. L. Vaughan, T. R. Healy, K. R. Bryan, A. D. Sneyd, and R. M. Gorman. Conservation, completeness and error in SPH fluids. *International Journal for Numerical Methods in Fluids*, 2008, Volume 56, Pages 37-62

[16] G. R. Johnson and S. R. Beissel. Normalised smoothing functions for SPH computation. *International Journal for Numerical Methods in Engineering*, 1996, Volume 39, Pages 2725-2741

[17] G. R. Johnson, R. A. Stryk, and S. R. Beissel. SPH for high velocity impact computations. *Computational Methods in Applied Mechanics and Engineering*, 139 34773, 1996

[18] T. Belytscho, Y. Krongauz, D. Organ, M. Fleming, and P. Krysl. Meshless methods: an overview and recent developments. *Computational Methods in Applied Mechanics and Engineering*, 139 (1996) 347

[19] T. Belytschko, Y. Krongauz, J. Dolbow, and C. Gerlach. On the completeness of meshfree particle methods. *International Journal for Numerical Methods in Engineering*, 1998, Volume 43, Pages 785-819

[20] N. Quinlan, M. Baba, and M. Lastiwka. An analysis of accuracy in one-dimensional smoothed particle hydrodynamics. 17th AIAA Computational Fluid Dynamics Conference 6 - 9 June 2005, Toronto, Ontario Canada

[21] L. D. Libersky and A. G. Petschek. Smooth particle hydrodynamics with strength of materials. *Advances in the Free Lagrange Method*, Lecture Notes in Physics, Vol. 395, Pages 248-257, 1990.

[22] I. Babuska. What I know and would like to know about The Meshless and Generalised FEM. University of Maryland Numerical Analysis Seminar, 2005, Workshop on Meshless Methods, Generalized Finite Element Methods, and Related Approaches, http://www.math.umd.edu/research/seminars/nas/meshless.html

[23] M. Zerroukat, K. Djidjeli, and A. Charafi. Explicit and implicit meshless methods for linear advection-diffusion-type partial differential equations. *International Journal of Numerical Methods in Engineering*, 2000, 48:19-35

[24] P. Laguna. Smoothed particle interpolation. *The Astrophysical Journal*, 439:814-821, 1995

[25] D. E. Grady and M. E. Kipp. Dynamic rock fragmentation. *Fracture Mechanics of Rock*, (New York: Academic) chapter 10, pp 42973, 1987

[26] W. Benz and E. Asphaug. Impact simulations with fracture: I. Method and tests. *Icarus*, 1233 98116, 1994

[27] J. J. Monaghan, R. F. Cas, A. Kos, and M. Hallworth. Gravity currents descending a ramp in a stratified tank. *Journal of Fluid Mechanics*, 379 369, 1999

[28] A. Colagrossi and M. Langrini. Numerical simulation of interfacial flows by smoothed particle hydrodynamics. *Journal of Computational Physics*, 191 44875, 2003

[29] T. Belytschko, Y. Y. Lu, and L. Gu. Element free Galerkin methods. *International Journal for Numerical Methods in Engineering*, Vol. 37, pp. 229-256, 1994

[30] T. Strouboulis, I. Babuška, and K. Copps. The design and analysis of the generalized finite element method. *Computer Methods in Applied Mechanics and Engineering Volume*, 181, Issues 1-3, 7 January 2000, Pages 43-6

[31] J. J. Monaghan. Why particle methods work. *SIAM Journal on Scientific and Statistical Computing*, Vol 3, No. 4, December 1982

[32] Jin Hongbin and Ding Xin. On criterions for smoothed particle hydrodynamics kernels in stable field. *Journal of Computational Physics*, 202 (2005) 699709, 2003

[33] R. Cabezn, D. Garca-Senz, and A. Relao. A one-parameter family of interpolating kernels for smoothed particle hydrodynamics studies. *Journal of Computational Physics*, 227 (2008) 85238540

[34] W. Hager. Condition estimates. *SIAM Journal on Scientific and Statistical Computing*, Volume 5, Issue 2, pp. 311-316 (June 1984)

[35] J. Bonet and S. Kulasegaram. A simplified approach to enhance the performance of smooth particle hydrodynamics methods. *Applied Mathematics and Computation*, 126 (2002) 133-155